Journal of Medicinal Chemistry

Article

Novel allosteric ligands of #-aminobutyric acid transporter 1 (GAT1) by MS based screening of pseudostatic hydrazone libraries

Tobias J. Hauke, Thomas Wein, Georg Höfner, and Klaus T. Wanner

J. Med. Chem., **Just Accepted Manuscript** • DOI: 10.1021/acs.jmedchem.8b01602 • Publication Date (Web): 30 Oct 2018

ACS Publications

is published by the American Chemical Society. 1155 Sixteenth Street N.W., Washington, DC 20036

Novel allosteric ligands of γ-aminobutyric acid transporter 1 (GAT1) by MS based screening of pseudostatic hydrazone libraries

*Tobias J. Hauke, Thomas Wein, Georg Höfner, Klaus T. Wanner**

Department of Pharmacy – Center of Drug Research, Ludwig-Maximilians-Universität München, Butenandtstr. 5–13, 81377 Munich, Germany

ABSTRACT

This study describes the screening of dynamic combinatorial libraries based on nipecotic acid as core structure with substituents attached to the 5- instead of the common 1-position for the search of novel inhibitors of the GABA transporter GAT1. The generated pseudostatic hydrazone libraries included a total of nearly 900 compounds and were screened for their binding affinities towards GAT1 in competitive mass spectrometry (MS) based binding assays. Characterization of the hydrazones with the highest affinities (with *cis*-configured *rac*-**16gf** bearing a 5-(1-naphthyl)furan-2-yl residue and a four atom spacer being the most potent) in binding and uptake experiments revealed an allosteric interaction at GAT1, which was not reported for any other nipecotic acid derivative up to now. Therefore, the herein introduced 5-substituted nipecotic acid derivatives could serve as valuable tools for investigations of allosterically modulated GABA transport mediated by GAT1, and furthermore as starting point for a new class of GAT1 inhibitors.

INTRODUCTION

γ-Aminobutyric acid (GABA; **1**; Chart 1) is the most important inhibitory neurotransmitter in the mammalian central nervous system (CNS) and pathological abnormalities of the GABAergic neurotransmission are associated with a number of neuronal diseases such as epilepsy,[1–3] Parkinson's disease,[3,4] depression[4,5] and neuropathic pain.[6,7] For the treatment of such diseases, GABAergic neurotransmission can be enhanced by agonists of GABA receptors, by targeting metabolic enzymes or by inhibiting GABA transport proteins (GATs).[8] With exception of one vesicular GABA transporter, GATs are membrane bound proteins encoded by the solute carrier 6 gene family (SLC6) that remove GABA from the synaptic cleft by utilizing a co-transport of sodium and chloride through cell membranes.[9] Amongst the four different subtypes of membrane bound transporters designated as GAT1, BGT1, GAT2 and GAT3 (as suggested by HUGO and corresponding to mGAT1, mGAT2, mGAT3 and mGAT4 when expressed in mice),[10,11] GAT1 is mainly responsible for the neuronal reuptake of GABA in the CNS and emerged as a drug target, while the pharmacological role and therapeutic potential of other GAT subtypes is still less well understood.[10–13] Many of the known GAT inhibitors are

derivatives of small cyclic amino acids such as nipecotic acid (**2**) and guvacine (**3**), which already show *in vitro* activity as GABA uptake inhibitors by their own.[14,15] By introducing a lipophilic side chain to the cyclic amino acids a new generation of inhibitors, represented by SK&F-89976A (**4**), tiagabine (**5**) or NO711 (**6**), was established that has an increased potency and selectivity towards GAT1 compared to unsubstituted amino acids.[16–19] Furthermore, the increased lipophilicity of those molecules (**4**–**6**) enabled them to cross the blood-brain barrier in contrast to the more hydrophilic, unsubstituted amino acids (**2**–**3**).[20] Tiagabine (**5**) is well characterized with respect to its anticonvulsant activity and it is the only selective GAT1 inhibitor in clinical use.[21] Recently, DDPM-2571 (**7**), a new GAT1 selective compound, was found to exceed the inhibitory potency of tiagabine (**5**) at GAT1 by more than one log unit and it was demonstrated to mediate anticonvulsant, anxiolytic, antidepressant and antinociceptive effects in mouse models.[22] All these selective and potent GAT1 inhibitors possess a hydrophilic amino acid “head” and a lipophilic aromatic moiety that is connected to the amino acid via a spacer originating from the amino nitrogen of the amino acid. There have been extensive efforts[23–29] to develop analogous GAT1 inhibitors with a different substitution pattern of the cyclic amino acid.

For example, 4-substituted nipecotic acid derivatives including compound *rac*-**8**[29] and 6-substituted guvacine derivatives including compound **9**[24] were synthesized and tested for their inhibitory potencies of the GABA transport. However, amongst these only compound **9** showed *in vitro* activity comparable to N-substituted derivatives, but was inactive in anticonvulsant models *in vivo*, likely due to an insufficient blood/brain concentration ratio.[24]

Chart 1. Structures of GABA (1), GAT1 inhibitors (2–9) and hypothetical molecule 10

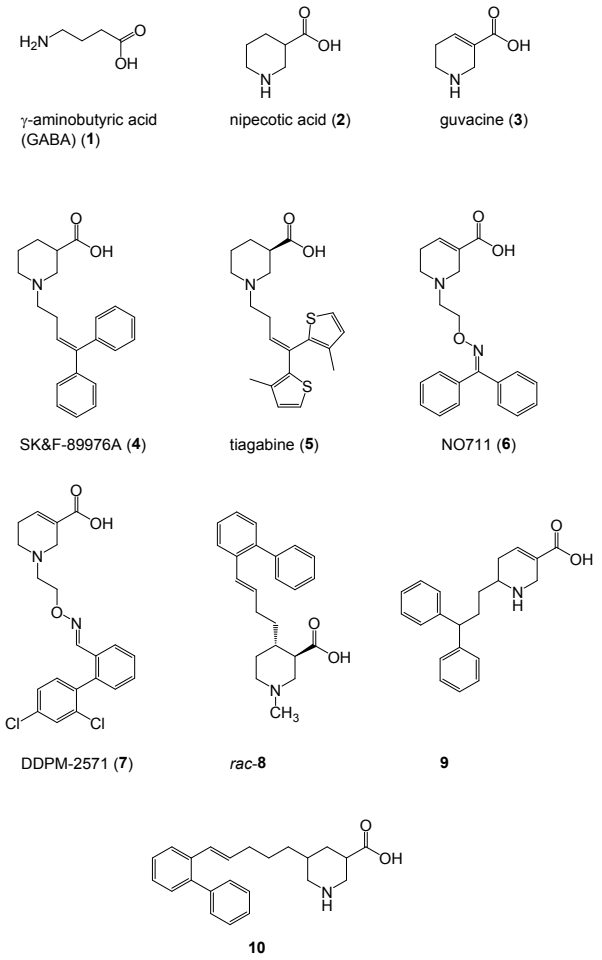

In 2005 the first crystal structure of a bacterial leucine transporter (LeuT) was reported,[30] which represents a homolog of the SLC6 GABA transporters. Since then, two

investigations used this structure as base for homology modeling and analysis of the binding of small inhibitors towards GAT1.[31,32] Later, the binding of tiagabine (**5**) and related compounds was evaluated using homology modeling, docking and molecular dynamics simulations[33] and different binding modes of small and large inhibitors were proposed.[34] We have used our in-house hGAT1 homology model refined by molecular dynamics calculations and described in detail in Wein et al.[34] to investigate the possibility of attaching the lipophilic arylalkyl residue to the 4- or 5-position of nipecotic acid (**2**). For an *in silico* screening we built a virtual library of 4- and 5-substituted nipecotic acid derivatives, of which the lipophilic residues were chosen to be biphenyl or diphenyl residues. For the linker, carbon chains with 3, 4, 5, or 6 atoms and bearing a double bond in conjugation with the aromatic moiety were examined (example see hypothetical molecule **10**). The substitution of nipecotic acid (**2**) particularly in the 5-position and with a five carbon spacer (as in molecule **10**) was found to achieve the highest docking scores amongst the hypothetical compounds. Docking calculations showed for nipecotic acid derivative **10** and related 5-substituted derivatives that the nitrogen atom was able to point towards the intracellular side of the binding cavity and could potentially interact with two

different hydrogen bond acceptors in this position. Thereby, the lipophilic residue would point to the extracellular side of the pocket (Figure 1c). So the binding pose of the piperidine ring of 5-substituted derivatives would be more similar compared to that of the unsubstituted nipecotic acid (**2**; Figure 1a) and opposing to that of tiagabine (**5**), of which the piperidine nitrogen and the attached arylalkyl moiety are facing towards the extracellular side (Figure 1b).[34]

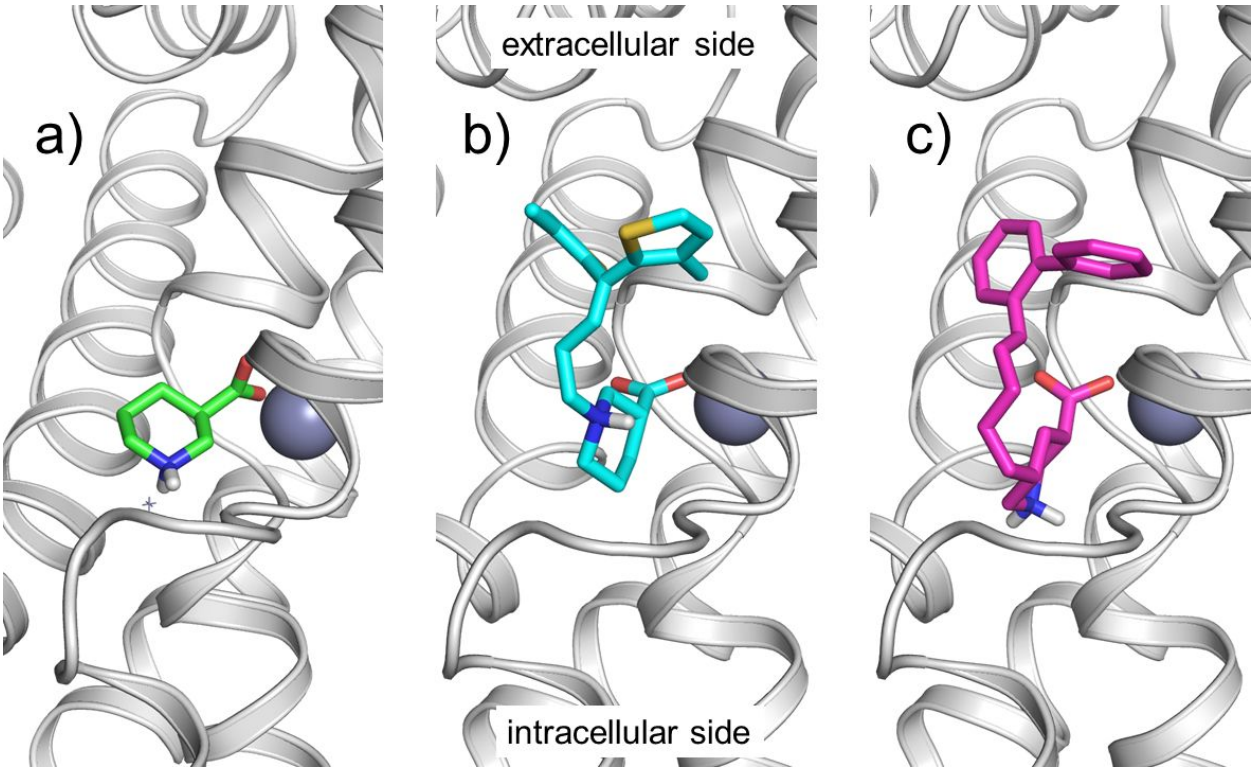

Figure 1. Side view of the hGAT1 model along the membrane plane showing the active site of the transporter. The extracellular side is on the top and the intracellular side is at the bottom of the picture. Docking poses of a) nipecotic acid (**2**; green), b) tiagabine (**5**; cyan) and c) hypothetical molecule **10** (magenta) in the molecular dynamics refined homology model of hGAT1 are shown. The transmembrane helices TM10, TM11 and TM12 are not displayed for clarity.

Based on these results obtained from *in silico* studies, we concluded that nipecotic derivatives bearing a lipophilic moiety attached to the 5-position via a spacer might possibly represent a new class of potent GABA uptake inhibitors. For a vast and most of all easy to perform variation of the structure of the lipophilic residues attached to the 5-position of the nipecotic acid moiety, we decided to analyze compound libraries generated by dynamic combinatorial chemistry (DCC). Hence, we followed an approach that is based on pseudostatic hydrazone libraries and uses a competitive mass spectrometry (MS) based binding assay for their analysis as reported from our group, recently.[35] MS Binding Assays have the advantage to enable the label-free determination of binding

affinities[36] and can be employed analogous to radioligand binding assays but are devoid of the drawbacks that result from using radioactive material.[37] The MS Binding Assay for the target murine GAT1 (mGAT1) that is required for this study and that uses NO711 (**6**) as a native marker had already been established by us and employed in related screening campaigns.[38]

For the present study we intended to synthesize nipecotic acid derivatives substituted at the 5-position with a C1 (*rac*-**11** and *rac*-**12**) and a C2 spacer (*rac*-**13** and *rac*-**14**) and with a hydrazine function at the end of the spacer. By reaction with appropriate aldehydes **15**, these nipecotic acid derived hydrazines should allow to generate libraries with a hydrazone function containing a total spacer length of four atoms (*rac*-**16** and *rac*-**17**; resulting from the conversion of hydrazines *rac*-**11** and *rac*-**12**) and five atoms (*rac*-**18** and *rac*-**19**; resulting from hydrazines *rac*-**13** and *rac*-**14**) (Scheme 1), which should be screened for their affinities towards mGAT1 and evaluated as potential GABA uptake inhibitors. Hence, compounds with a five atom spacer, as suggested by molecular modeling, as well as with a four atom spacer, which appeared beneficial in some

previously reported cases when potentially new N-substituted GAT1 inhibitors were synthesized,[39,40] should be examined in this study.

Scheme 1. Condensation of nipecotic acid derived hydrazines *rac*-11–*rac*-14 with diverse aldehydes 15 to afford hydrazones with general structures *rac*-16–*rac*-19

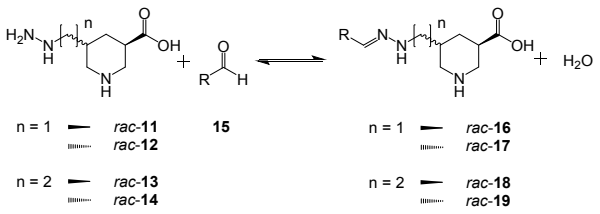

In addition to the generation and screening of the hydrazone libraries in competitive binding assays the whole screening process would further comprise deconvolution of the most potent libraries (testing only single hydrazones) and hit verification by resynthesis and determination of pK_i values. Finally, the best binders should be tested in [^{3}H]GABA uptake assays for their functional activity (IC_{50}) and subtype selectivity.

RESULTS AND DISCUSSION

Chemistry.

Synthesis of hydrazines. For the synthesis of the desired hydrazines (*rac*-**11**–*rac*-**14**) a carbon side chain had to be introduced in the 5-position of nipecotic acid (or derivatives thereof) exhibiting a terminal function suitable for further derivatization, i.e. the introduction of a hydrazine moiety. As common precursors required for all hydrazine derivatives, the aldehydes *rac*-**20** and *rac*-**21** were chosen. These aldehydes were synthesized from commercially available nicotinate **22** as shown in Scheme 2. Compounds *rac*-**23** and *rac*-**24** were obtained by a hydrogenation of nicotinate **22** and a subsequent protection of the amino function with a *tert*-butyloxycarbonyl (Boc) group. To this end, conditions as described in a patent[41] were applied initially. However, under these conditions the hydrogenation reaction did not lead to a conversion of the starting material (**22**). Accordingly, the procedure was modified by adding sulfuric acid to the reaction mixture in the hydrogenation step. With this modified protocol the two diastereomeres *rac*-**23** and *rac*-**24** (in 3:1 ratio) were obtained in yields of 55% (*rac*-**23**) and 19% (*rac*-**24**) after separation by flash chromatography. The major diastereomere *rac*-**23** was oxidized with Dess-Martin periodinane analogous to a patent[42] yielding the ketone **25** (74%; the

oxidation of the two diastereomeres *rac*-**23** and *rac*-**24** as a mixture afforded **25** in approximately the same yield).

Scheme 2. Synthesis of nipecotic acid derived hydrazines with C1 spacer (*rac*-11 and *rac*-12) and C2 spacer (*rac*-13 and *rac*-14)[a]

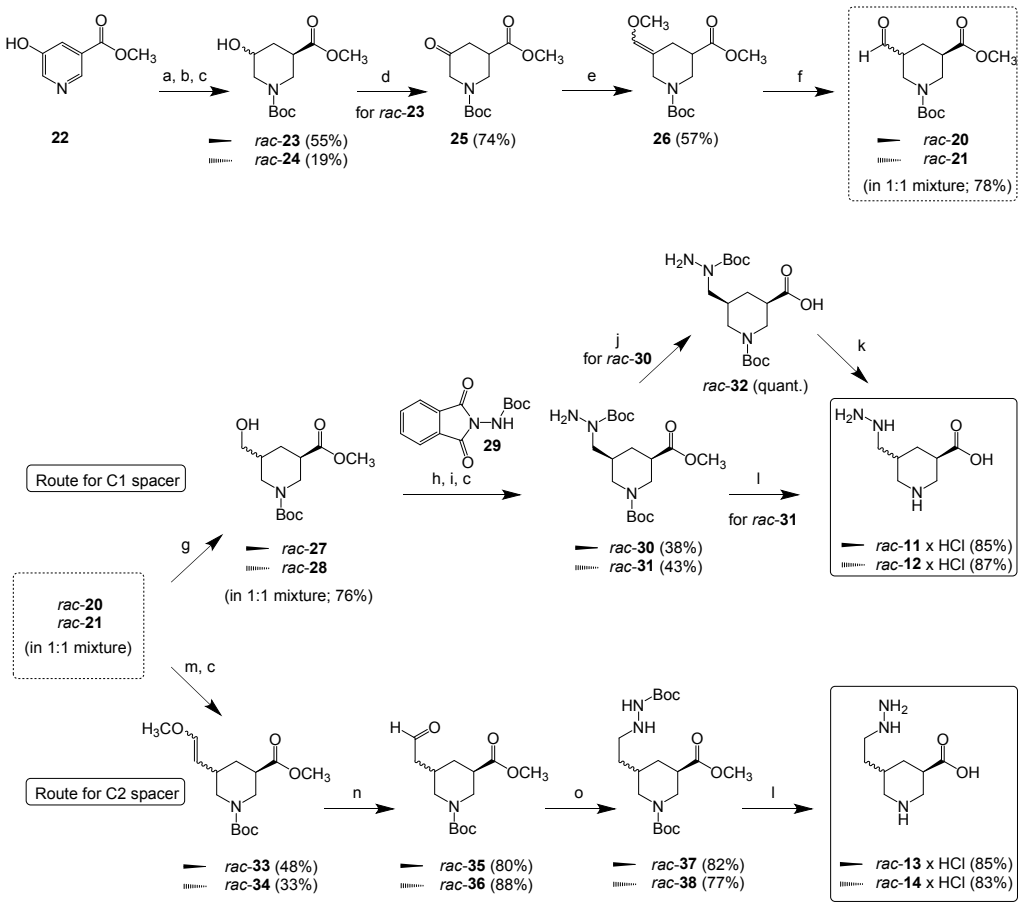

[a]Reagents and conditions: (a) H_2 (10 bar), Rh/Al_2O_3, H_2SO_4, MeOH, 80 °C, 16 h; (b) Boc_2O, NEt_3, dioxane, rt, 3 h; (c) separation of diastereomeres by flash chromatography; (d) Dess-Martin periodinane, DCM, rt, 2.5 h; (e) $Ph_3PCH_2OCH_3Cl$, *t*-BuOK, THF, -78

°C→rt, 2 h; (f) aq. HCl (2 M), THF, 0 °C→rt, 2 d; (g) $NaBH_4$, EtOH, 0 °C, 1 h; (h) PPh_3, DIAD, **29**,[47] THF, 0 °C, 105 min; (i) CH_3NHNH_2, THF, 0 °C, 2 h; (j) aq. NaOH (1 M), MeOH, 0 °C→rt, 15 h; (k) HCl in Et_2O (2 M), rt, 3 d; (l) aq. HCl (1 M), H_2O, 60 °C (sealed high-pressure tube), 3 h; (m) $Ph_3PCH_2OCH_3Cl$, *t*-BuOK, THF, 0 °C→rt, 1.5 h; (n) aq. HCl (2 M), THF, 0 °C→rt, 7–9 h; (o) Boc-$NHNH_2$, NaH_3BCN, AcOH, MeOH, 0 °C→rt, 2.5–3.5 h.

To introduce the side chain in the 5-position of **25** we performed a Wittig reaction (analogously as it was described in literature for different compounds)[43] with the ylide generated from methoxymethyl triphenylphosphonium chloride by means of potassium *tert*-butoxide which yielded the enol ether **26** (57%; 1:1 mixture of *E*- and *Z*-isomer; isomers not separated). The hydrolysis of the enol ether group was accomplished by a modified protocol for an analogous reaction from literature[43] using 2 M HCl (instead of 4 and 6 M) and a higher proportion of the solvent THF (6:1 instead of 1:1 of THF/acid). That way the undesired additional hydrolysis of the ester function could be reduced and diastereomeric aldehydes *rac*-**20**[44] and *rac*-**21** could be obtained in a yield of 78% as a

1:1 mixture, the separation of which appeared to be laborious due to their nearly identical chromatographic retention.

For the synthesis of the nipecotic acid derived hydrazine derivatives with a C1 spacer, *rac*-**11** and *rac*-**12**, at first a direct reductive hydrazine formation was attempted by converting the mixture of aldehydes *rac*-**20** and *rac*-**21** with *tert*-butyl carbazate applying different reducing agents (e.g. sodium cyanoborohydride or sodium borohydride). This, however, did not lead to the desired Boc-protected hydrazine derivatives. As an alternative, the introduction of the required hydrazine function should be accomplished by a Mitsunobu reaction following a protocol of Brosse et al.[45-47] Alcohols *rac*-**27**[44] and *rac*-**28**[48] required for this purpose were prepared by reduction of aldehydes *rac*-**20** and *rac*-**21** (in 1:1 mixture) with sodium borohydride (*rac*-**27** and *rac*-**28**; 1:1 mixture; 76%). The thus obtained 1:1 mixture of *rac*-**27** and *rac*-**28** (yield 76%) was treated with hydrazine derivative **29**,[47] triphenylphosphine and diisopropyl azodicarboxylate (DIAD) in a Mitsunobu reaction. The formed product was subsequently freed from the phthalimide protecting group with methylhydrazine yielding the hydrazine precursors *rac*-**30** and *rac*-**31** in good yields (38% and 43%, respectively) after separation with flash

chromatography. Target compound *rac*-**12** as hydrochloride[49] was finally obtained in good yield (87%) by simultaneous hydrolysis of the ester function and cleavage of the Boc group of *rac*-**31** by heating to 60 °C in aqueous HCl and in a sealed high-pressure tube. The same procedure applied to *rac*-**30**, however, did not lead to the pure product *rac*-**11**. Instead a mixture of *rac*-**11** with a side product was obtained, which presumably resulted from an intramolecular cyclization reaction of the hydrazine moiety with the carboxylic acid ester function. Hence, the procedure was modified. To avoid the undesired cyclization reaction, the deprotection of the functional groups was performed in two steps. First, the ester was hydrolyzed with NaOH to give the free acid *rac*-**32** and then the Boc groups were cleaved in etheric HCl, giving the desired *rac*-**11** as hydrochloride[49] in good yield (85% over two steps).

For the preparation of nipecotic acid derivatives with the hydrazine function attached to a C2 spacer, we performed the Wittig reaction with aldehydes *rac*-**20** and *rac*-**21** analogous as for the synthesis of the enol ether **26**. The two diastereomeric enol ethers, *rac*-**33** and *rac*-**34**, could be isolated by flash chromatography in pure form (*rac*-**33**; 48% and *rac*-**34**; 33%). The enol ether hydrolysis of the individual diastereomeres proceeded more

smoothly than with the analogs with shorter side chains, giving aldehydes *rac*-**35** and *rac*-**36** in yields of 80% and 88%. When reacted with *tert*-butyl carbazate in the presence of sodium cyanoborohydride and acetic acid following an analogous literature method[50] the Boc-protected hydrazines *rac*-**37** and *rac*-**38** were obtained in good yields (85% and 83%, respectively). The protective groups in *rac*-**37** and *rac*-**38** (Boc and ester function) could finally be removed in one step by heating the compounds in hydrochloric acid to 60 °C in a sealed high-pressure tube. The hydrochlorides of the desired nipecotic acid derived hydrazines with C2 spacer, *rac*-**13** and *rac*-**14**,[49] were thus obtained in yields of 85% and 83%, respectively.

Aldehydes. Aldehydes **15a**–**15hp** (Chart 2), required for library generation, were mostly purchased from commercial suppliers and some synthesized by literature methods.[51,52] Aldehydes **15fd**, **15ff**, **15fh**, **15fi**, **15fn**, **15fp**, **15fs** and **15gr** were synthesized in a Suzuki-Miyaura reaction[51,53] (see Supporting Information). Following previous approaches,[35,51,52] preferentially lipophilic, aromatic aldehydes were included in the libraries taking into account known structure-activity relationships for benchmark GAT inhibitors typically possessing a polar core structure (mostly an amino acid), a spacer of variable length and

aromatic moieties (see compounds **4**–**9**). New aldehydes were added in the order of their availability.

Synthesis of hydrazones. For the hit verification individual hydrazones, *rac*-**16** or *rac*-**18**, were separately synthesized by combining 1.0 equivalent of hydrazine, *rac*-**11** x HCl or *rac*-**13** x HCl, with 1.0 equivalent of aldehyde **15** as shown in Scheme 1. Additionally, stoichiometric amounts of NaOD were added to neutralize HCl, introduced with the hydrazines.[49] For practical reasons the reactions were performed in deuterated solvents (DMSO-d_6/D_2O = 9:1) to be able to monitor reaction progress by NMR.[54]

General aspects of library generation.

The generation and screening of the hydrazone libraries delineated from hydrazine derivatives *rac*-**11**–*rac*-**14**, the synthesis of which was described above, should be accomplished analogous to a method recently published by us.[35]

In that case, a nipecotic acid derivative provided with a hydrazine function attached to the N-atom via a linker was incubated with aldehyde libraries, each library containing four constituents. For the sake of simplicity hydrazone library formation was performed in the

presence of the target, mGAT1. The incubation time was set to four hours, which was found sufficient for a complete conversion, and the pH adjusted to 7.1 being compatible with the presence of the proteins. The hydrazine was applied in excess (100 μM) compared to the aldehydes (four different aldehydes, concentration of each 10 μM) in order to render composition of the libraries constant, pseudostatic, though they are still dynamic. To determine the activity of the libraries, the incubation mixtures were directly used for competitive MS binding experiments. To this end, the MS marker NO711 (**6**) was directly added to the incubation mixture. After additional 40 min of incubation, the amount of specifically bound MS marker **6**, which is serving as a measure of the activity of the library (after liberation from the target), was quantified by LC-ESI-MS/MS.

Basically, for the present study the experimental conditions were analogous to those in the initial approach as well as in a second subsequent application.[35,51] Hence, libraries were generated in the presence of the target mGAT1 and their activities were then analyzed by competitive MS Binding Assays as described above. However, the following changes were made: The library size was increased from four to eight (aldehydes per library) and the concentration of individual aldehydes was set to 1.0 μM. Finally, a library

containing eight constituents in a concentration of 1 μM should be considered “active”, if it reduced the amount of bound MS marker to < 50%. Provided the activity of a library (i.e. the reduction of MS marker binding to < 50%) was due to a single component, the affinity of this binder (IC_{50} value) should be at least 1 μM or lower. Besides, the concentration of the hydrazine derivatives *rac*-**11**–*rac*-**14** was raised to 200 μM as hydrazine concentrations of 100 μM (as in previous approaches)[35,51] did not lead to a complete hydrazone formation within the given incubation period (see Supporting Information). Hence, the 25-fold amount of hydrazines (*rac*-**11**–*rac*-**14**) as compared to total aldehyde concentration was applied for hydrazone library generation in the present study.

Chart 2. Libraries consisting of aldehydes 15a–15hp

aldehyde library 1

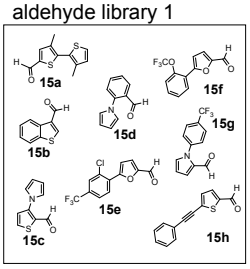

aldehyde library 2

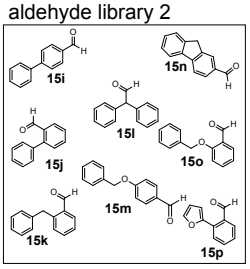

aldehyde library 3

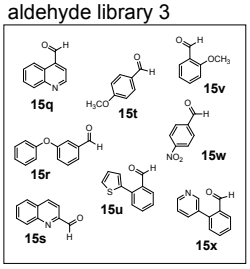

aldehyde library 4

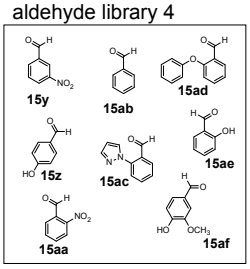

aldehyde library 5

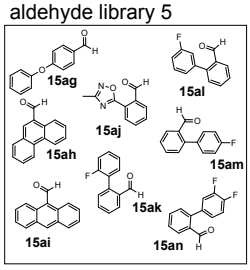

aldehyde library 6

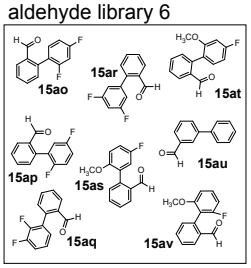

aldehyde library 7

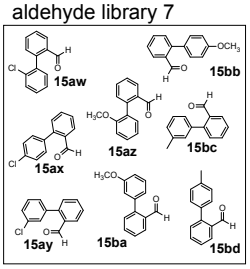

aldehyde library 8

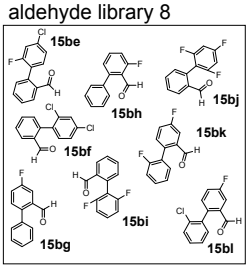

aldehyde library 9

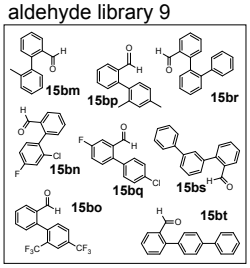

aldehyde library 10

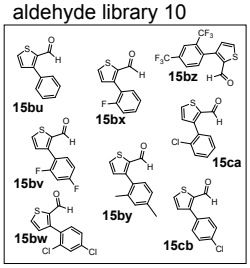

aldehyde library 12

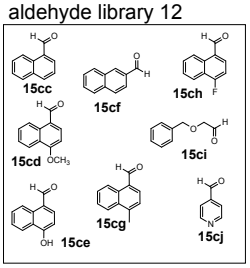

aldehyde library 12

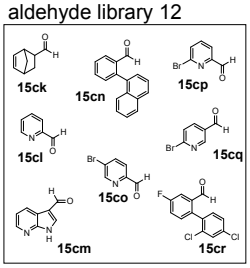

aldehyde library 13

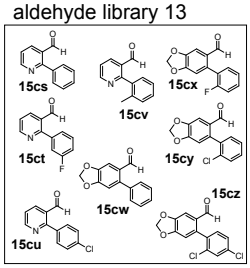

aldehyde library 14

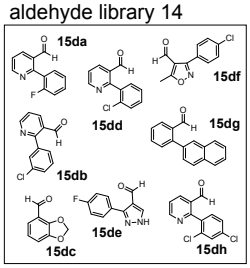

aldehyde library 15

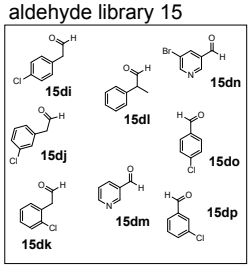

aldehyde library 16

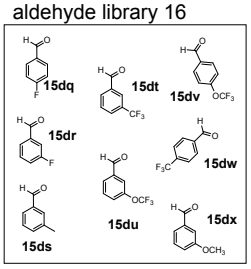

aldehyde library 17

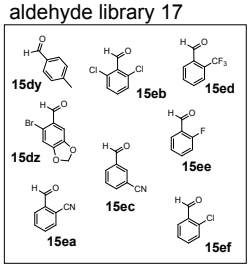

aldehyde library 18

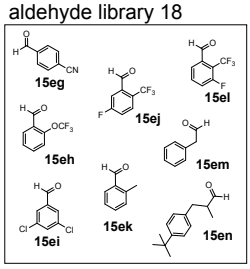

aldehyde library 19

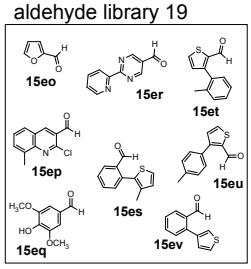

aldehyde library 20

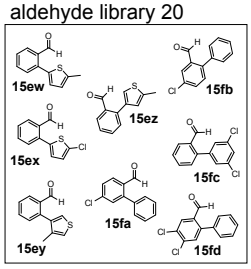

aldehyde library 21

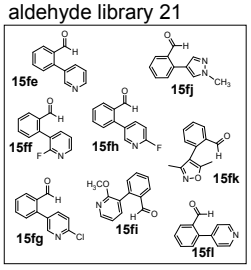

aldehyde library 22

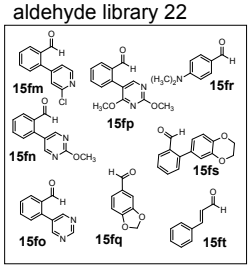

aldehyde library 23

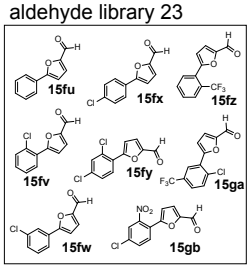

aldehyde library 24

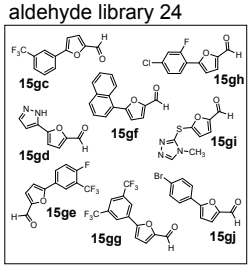

aldehyde library 25

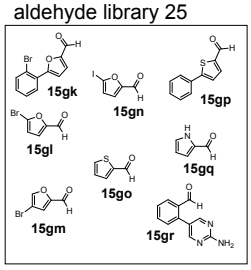

aldehyde library 26

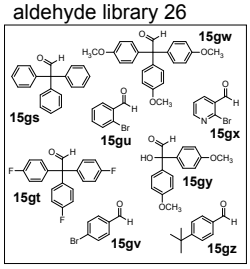

aldehyde library 27

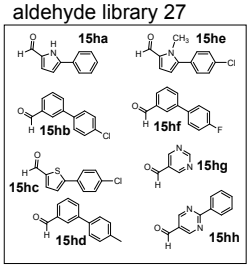

aldehyde library 28

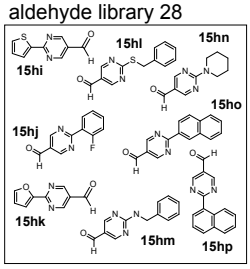

Screening and deconvolution of hydrazone libraries.

In the present study a total of 224 aldehydes grouped in 28 libraries, each containing eight individual aldehydes in a concentration of 1.0 μM, were used (Chart 2). Each of the 28 aldehyde libraries was converted with all four hydrazines (*rac*-**11**–*rac*-**14**; applied as hydrochlorides;[49] 200 μM) in separate experiments into the corresponding libraries of hydrazones (Scheme 3). In the following hydrazone libraries are termed "*cis*-C1", "*trans*-C1", "*cis*-C2" and "*trans*-C2" for hydrazones derived from *rac*-**16**, *rac*-**17**, *rac*-**18** and *rac*-**19**, respectively, thus indicating their relative configurations and different spacer lengths.

Scheme 3. Example for the conversion of aldehyde library 1 with hydrazine *rac*-11 into *cis*-C1 hydrazone library 1

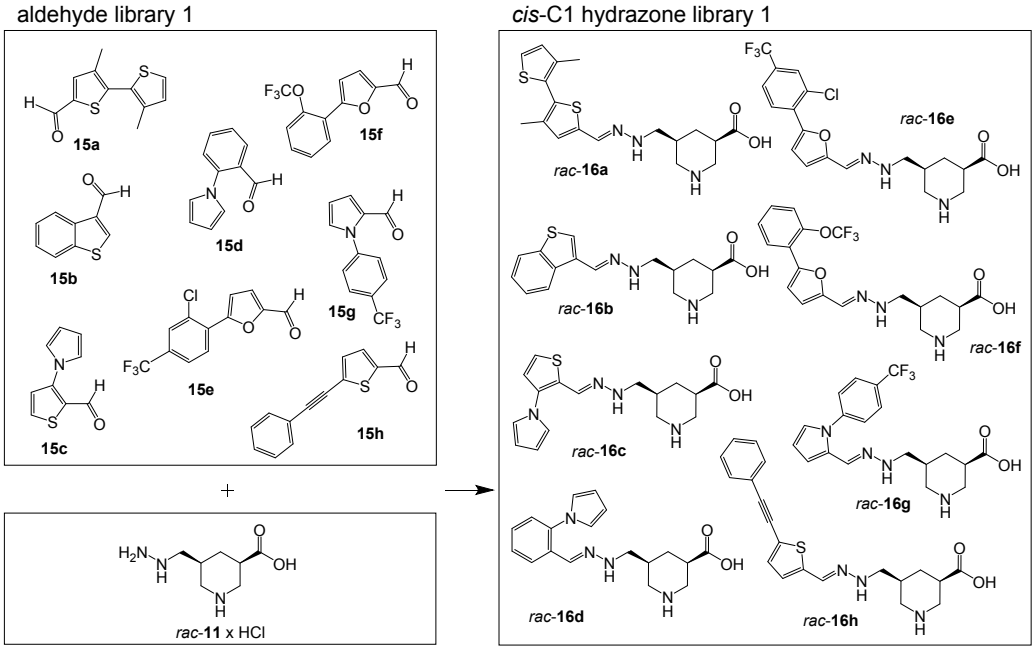

The results of the screening experiments for the hydrazone libraries are shown in Figure 2. Control experiments with the aldehyde libraries 1–28 (aldehydes **15a**–**15hp**) and hydrazines *rac*-**11**–*rac*-**14** alone were performed to ensure that in the applied concentrations none of the building blocks affected the marker binding to a remarkable extent (see Supporting Information).

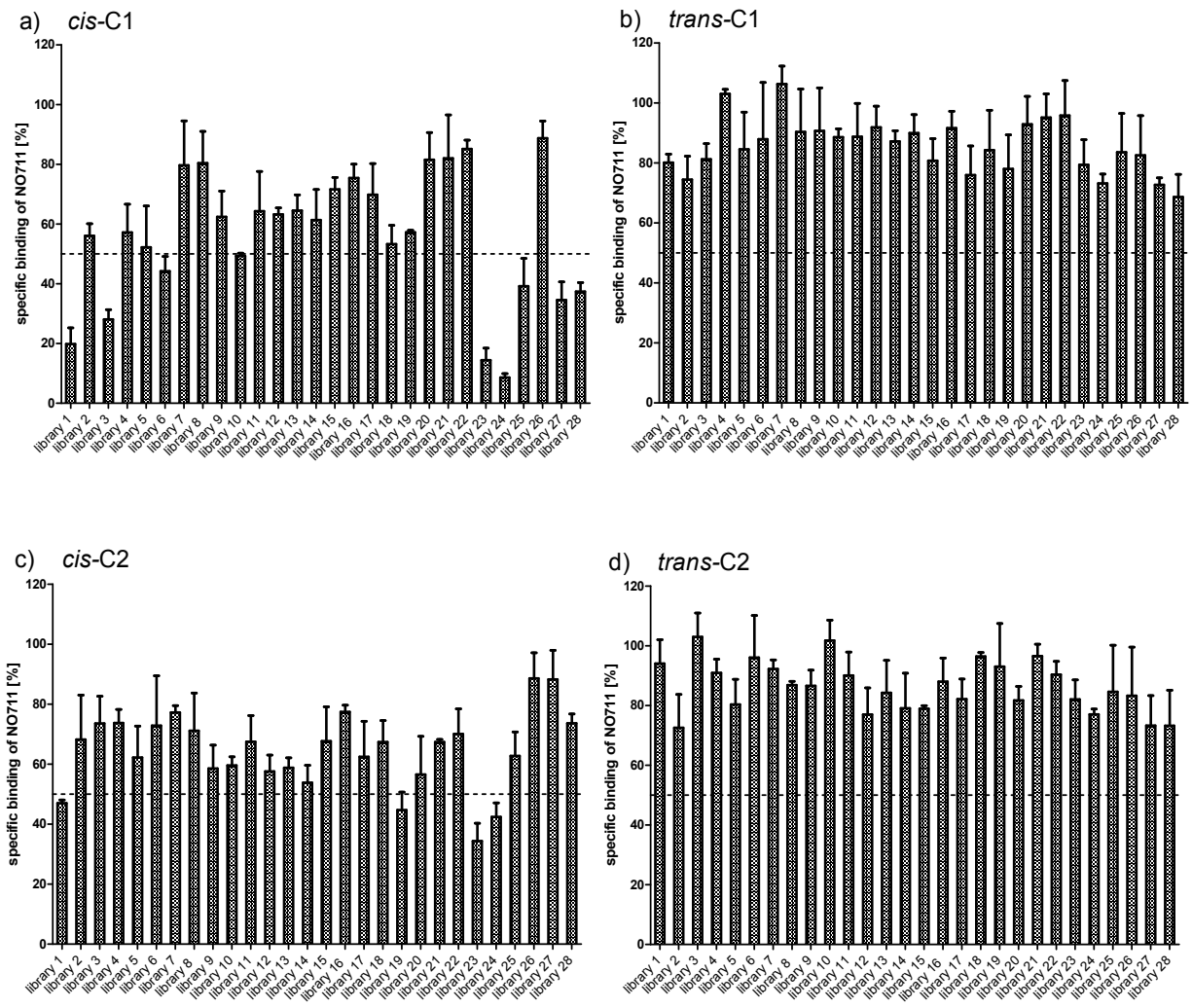

Figure 2. Screening of a) *cis*-C1 (*rac*-**16**), b) *trans*-C1 (*rac*-**17**), c) *cis*-C2 (*rac*-**18**) and d) *trans*-C2 hydrazone libraries (*rac*-**19**). The bars indicate the percentage of remaining specific binding of NO711 (**6**) after an incubation time of 4 h for library generation and 40 min for marker binding to mGAT1; data represent means±SD of four replicates. The limit for further analysis of a library was defined as 50% remaining marker binding (indicated by the dashed line).

Nine *cis*-C1 hydrazone libraries (*rac*-**16**; libraries 1, 3, 6, 10, 23, 24, 25, 27 and 28; Figure 2a) and four *cis*-C2 hydrazone libraries (*rac*-**18**; libraries 1, 19, 23 and 24; Figure 2c) were found to reduce the remaining MS marker binding below 50% (by mean values of four replicates) and thus were considered active. Interestingly, all active libraries derived from *cis*-configured nipecotic acid derivatives, while the *trans*-C1 (*rac*-**17**; Figure 2b) and *trans*-C2 hydrazone libraries (*rac*-**19**; Figure 2d) did not show any striking activity towards mGAT1. All of the 13 hydrazone libraries considered active were further examined in deconvolution experiments in order to identify their most active components. For these experiments single hydrazones were studied in the same way as the libraries except that only single aldehydes were employed in the test procedure (incubation of aldehydes in a concentration of 1.0 μM with hydrazine *rac*-**11** and *rac*-**13**, respectively, in a concentration of 200 μM). As summarized in Table 1, 16 hydrazones reduced MS marker binding below the set limit of 50%, while none of the corresponding aldehydes alone showed remarkable activity. 14 of the active compounds were represented by the shorter chained hydrazones *rac*-**16**, showing remaining MS marker binding of 16–49% (*rac*-**16e**, *rac*-**16r**, *rac*-**16fv**, *rac*-

16fw, *rac*-**16fy**, *rac*-**16fz**, *rac*-**16ga**, *rac*-**16gb**, *rac*-**16gc**, *rac*-**16ge**, *rac*-**16gf**, *rac*-**16gg**, *rac*-**16gk** and *rac*-**16ho**; Table 1, entries 5, 10, 42–43, 45–49, 51–53, 57 and 79). Amongst the longer chained derivatives only hydrazones *rac*-**18e** and *rac*-**18fy** fulfilled the criterion for further analysis by reducing MS marker binding to 47% and 41%, respectively (Table 1, entries 5 and 45). As mentioned above, with a reduction of the marker binding to 50% or lower when applied in a concentration of 1 µM, "active" test compounds should correspond to a maximum IC_{50} of 1 µM. Thus, we considered it worth to subject all these 16 hydrazones to further analysis.

Table 1. Results of the deconvolution experiments for "active" hydrazone libraries

entry	library	compd 15/*rac*-16/*rac*-18	specific binding of NO711 [%][a] aldehyde 15	*cis*-C1 (*rac*-16)	*cis*-C2 (*rac*-18)	entry	library	compd 15/*rac*-16/*rac*-18	specific binding of NO711 [%][a] aldehyde 15	*cis*-C1 (*rac*-16)	*cis*-C2 (*rac*-18)
	library						library				
1	1	-a	106±6	74±8	79±6	41	23	-fu	82±16	68±6	61±9
2		-b	77±18	82±4	75±10	42		-fv	99±14	48±4	52±11
3		-c	82±17	86±9	72±6	43		-fw	103±9	46±6	69±14
4		-d	92±11	91±5	82±2	44		-fx	75±12	56±2	62±11
5		-e	98±4	40±2	47±4	45		-fy	97±8	40±7	41±5
6		-f	88±25	66±10	59±13	46		-fz	90±12	49±9	60±6
7		-g	87±21	75±5	74±14	47		-ga	88±13	38±4	54±4
8		-h	90±16	51±6	71±10	48		-gb	72±4	37±3	60±6
	library						library				
9	3	-q	100±14	74±15	-	49	24	-gc	70±5	38±2	70±4

10		**-r**	109±11	46±10	-	50		**-gd**	93±10	81±11	72±8
11		**-s**	114±6	81±1	-	51		**-ge**	99±3	36±2	72±7
12		**-t**	98±23	85±3	-	52		**-gf**	92±12	16±1	58±13
13		**-u**	107±10	87±3	-	53		**-gg**	103±18	32±1	76±4
14		**-v**	108±12	85±6	-	54		**-gh**	97±9	67±9	64±14
15		**-w**	113±12	83±14	-	55		**-gi**	86±15	84±11	73±4
16		**-x**	119±6	93±6	-	56		**-gj**	97±6	59±2	65±9
	library						library				
17	6	**-ao**	97±3	66±15	-	57	25	**-gk**	129±3	36±6	-
18		**-ap**	98±11	73±11	-	58		**-gl**	127±5	55±13	-
19		**-aq**	107±7	58±3	-	59		**-gm**	126±4	53±13	-
20		**-ar**	112±10	90±11	-	60		**-gn**	115±10	69±6	-
21		**-as**	108±13	72±11	-	61		**-go**	118±3	67±8	-
22		**-at**	101±11	80±9	-	62		**-gp**	112±15	55±3	-
23		**-au**	111±11	52±2	-	63		**-gq**	107±10	89±4	-
24		**-av**	112±2	70±15	-	64		**-gr**	121±5	93±4	-
	library						library				
25	10	**-bu**	113±7	85±2	-	65	27	**-ha**	98±7	85±7	-
26		**-bv**	118±5	80±13	-	66		**-hb**	108±17	52±10	-
27		**-bw**	116±9	81±16	-	67		**-hc**	107±18	75±6	-
28		**-bx**	121±7	84±8	-	68		**-hd**	104±26	61±7	-
29		**-by**	124±17	80±7	-	69		**-he**	101±5	87±16	-
30		**-bz**	129±6	88±3	-	70		**-hf**	122±10	50±7	-
31		**-ca**	121±15	84±6	-	71		**-hg**	118±8	64±12	-
32		**-cb**	113±8	80±13	-	72		**-hh**	113±19	55±7	-
	library						library				
33	19	**-eo**	107±15	-	60±7	73	28	**-hi**	103±15	60±15	-
34		**-ep**	103±1	-	62±5	74		**-hj**	116±9	68±11	-
35		**-eq**	99±10	-	62±20	75		**-hk**	118±7	73±12	-
36		**-er**	106±9	-	83±5	76		**-hl**	116±15	53±5	-
37		**-es**	105±12	-	61±15	77		**-hm**	118±2	60±3	-
38		**-et**	93±17	-	64±14	78		**-hn**	108±21	69±11	-
39		**-eu**	109±3	-	83±10	79		**-ho**	110±11	27±4	-
40		**-ev**	106±2	-	80±4	80		**-hp**	124±3	61±13	-

[a]Percentage of remaining specific binding of NO711 (**6**) in the presence of either pure aldehyde **15** or *cis*-C1 (*rac*-**16**) or *cis*-C2 hydrazones (*rac*-**18**) after an incubation time of 4 h for hydrazone formation and 40 min for marker binding to mGAT1; data represent means±SD of four replicates. The limit for further analysis of a hydrazone was defined as 50% remaining marker binding (hydrazones considered active are highlighted in yellow).

Hit verification.

For hit verification the 16 hydrazones found most active in deconvolution experiments were synthesized in pure form and their binding affinities (pK_i values) were established in full-scale competitive MS binding experiments.

Table 2. Binding affinities (pK_i) determined in competitive binding assays at mGAT1 of hydrazones synthesized in pure form

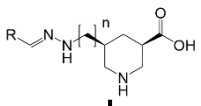

entry	compd[a]	n	R	pK_i[b,c]	entry	compd[a]	n	R	pK_i[b,c]
1	*rac*-**16e**	1	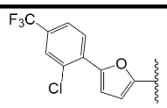	6.35±0.02	9	*rac*-**16gc**	1	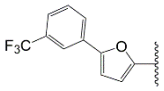	6.15±0.01
2	*rac*-**16r**	1	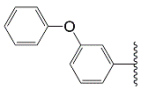	6.02±0.11	10	*rac*-**16ge**	1	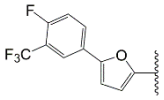	5.90±0.04
3	*rac*-**16fv**	1	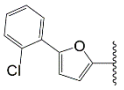	5.91±0.08	11	*rac*-**16gf**	1	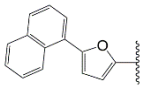	6.67±0.03
4	*rac*-**16fw**	1	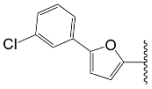	5.73±0.10	12	*rac*-**16gg**	1	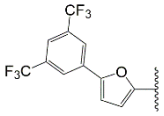	6.61±0.00
5	*rac*-**16fy**	1	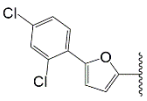	6.19±0.05	13	*rac*-**16gk**	1	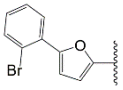	5.84±0.09

6	*rac*-**16fz**	1	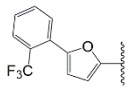	5.64±0.14	14	*rac*-**16ho**	1	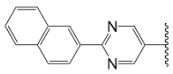	6.03±0.06
7	*rac*-**16ga**	1	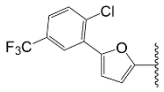	6.33±0.11	15	*rac*-**18e**	2	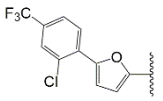	6.21±0.08
8	*rac*-**16gb**	1	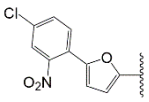	5.83±0.09	16	*rac*-**18fy**	2	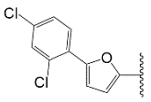	6.32±0.05

[a]Individually synthesized from appropriate aldehydes and hydrazines, see also reference.[54] [b]pK_i values are given as means±SEM of three independent experiments. [c]Tiagabine (**5**) was used as reference in all experiments and a pK_i of 7.56±0.06 (n = 8) was found for this compound.

The pK_i values found for the hydrazones are in a range from 5.64 to 6.67 (Table 2). The binding affinities of the best 5-substituted nipecotic acid derived hydrazones (e.g. *rac*-**16gf**; Table 2, entry 11 or *rac*-**16gg**; Table 2, entry 12) are almost as good as those of yet established potent GAT1 inhibitors such as tiagabine (**5**; pK_i = 7.56) with the difference in the nominal pK_i values being only about one log unit.

Among the best binders from this study one possesses a 3-phenoxyphen-1-yl (*rac*-**16r**; pK_i = 6.02; Table 2, entry 2), another a 2-(2-naphthyl)pyrimidin-5-yl (*rac*-**16ho**; pK_i = 6.03;

Table 2, entry 14) residue. All other compounds are characterized by the presence of a 5-arylfuran-2-yl residue. Thereby, the furanyl moiety is linked to differently substituted phenyl residues or to a naphthyl residue. The hydrazone *rac*-**16gf** (pK_i = 6.67; Table 2, entry 11) bearing a 5-(1-naphthyl)furan-2-yl residue showed the highest binding affinity towards mGAT1 amongst all hydrazones in this study. For compounds with a 5-phenylfuran-2-yl residue mono-substituted at the phenyl ring, a chlorine atom in *ortho*-position gives rise to a binding affinity (*rac*-**16fv**; pK_i = 5.91; Table 2, entry 3) nominally slightly superior to that with a chlorine atom in *meta*-position (*rac*-**16fw**; pK_i = 5.73; Table 2, entry 4), while a trifluoromethyl substituent gives rise to a higher affinity in *meta*- (*rac*-**16gc**; pK_i = 6.15; Table 2, entry 9) than in *ortho*-position (*rac*-**16fz**; pK_i = 5.64; Table 2, entry 6). Compound *rac*-**16gk** (pK_i = 5.84; Table 2, entry 13) with a bromine atom in *ortho*-position of the phenyl ring showed a similar binding affinity as its chloro analog *rac*-**16fv** (pK_i = 5.91; Table 2, entry 3). Except for compounds *rac*-**16gb** with an *ortho*-nitro and a *para*-chloro substituted phenyl ring (pK_i = 5.83; Table 2, entry 8) and *rac*-**16ge** with a *meta*-trifluoromethyl and a *para*-fluoro substitution (pK_i = 5.90; Table 2, entry 10) a second substituent (i.e. chloro or trifluoromethyl) at the phenyl ring was generally favorable

leading to pK_i values in a range of 6.19 to 6.61 (for *rac*-**16e**, *rac*-**16fy**, *rac*-**16ga**, *rac*-**16gg**, *rac*-**18e** and *rac*-**18fy**). The hydrazone *rac*-**16gg** (pK_i = 6.61; Table 2, entry 12) bearing a 3,5-di(trifluoromethyl)phen-1-ylfuran-2-yl residue was found to be the best binder amongst all disubstituted phenyl moieties and in total second best after naphthylfuranyl derivative *rac*-**16gf** amongst all hydrazones. The shorter spacer length as in hydrazones *rac*-**16** (4 atoms) appears to be more favorable than the longer one in *rac*-**18** (5 atoms), as amongst *cis*-C1 hydrazones (*rac*-**16**) as compared to *cis*-C2 hydrazones (*rac*-**18**) more compounds fulfilling the activity criteria were found with higher affinities (pK_i = 6.67 for *rac*-**16gf** versus pK_i = 6.32 for *rac*-**18fy**). Still, with pK_i values of 6.21 (*rac*-**18e**; Table 2, entry 15) and 6.32 (*rac*-**18fy**; Table 2, entry 16) certain *cis*-C2 hydrazones (*rac*-**18**) also showed good binding affinities towards mGAT1 and their pK_i values are similar to the ones of their direct (i.e. possessing the same lipophilic moieties) shorter-spaced analogs *rac*-**16e** (pK_i = 6.35; Table 2, entry 1) and *rac*-**16fy** (pK_i = 6.19; Table 2, entry 5).

Interestingly, none of the evaluated hydrazones possesses an *ortho*-biphenyl residue as lipophilic domain which was found to play a dominant role amongst the best binders from our previous library screening approaches focusing on nipecotic acid derivatives with the

lipophilic arylalkyl domain being attached to the amino funcion.[35,51,52] Instead, the described screening of pseudostatic DCC libraries of 5-substituted nipecotic acid derivatives revealed mGAT1 ligands with good binding affinities exhibiting lipophilic aromatic moieties so far unprecedented for this type of bioactive compounds: The 3-phenoxyphenyl, 2-(2-naphthyl)pyrimidin-5-yl, 5-(1-naphthyl)furan-2-yl and 5-phenylfuran-2-yl residue. Notably, the latter showed its highest binding affinities when the phenyl moiety was substituted with chloro or trifluoromethyl substituents. In case of the other three moieties no corresponding substituted aldehydes were available that could have been included in the screening process.

After characterization of the binding affinities (pK_i values) we examined the functional activities, i.e. the inhibitory potencies (pIC_{50} values), at the four GABA transporter subtypes for the six best binders, *rac*-**16e**, *rac*-**16ga**, *rac*-**16gf**, *rac*-**16gg**, *rac*-**18e**, *rac*-**18fy**. The results obtained in [^{3}H]GABA uptake assays with HEK cells stably expressing mGAT1–mGAT4[55] are summarized in Table 3. The pIC_{50} values at mGAT1 are in a range from 4.09 to 4.64 except for compound *rac*-**16gg**, which did not show an inhibitory potency high enough for reliable determination of a pIC_{50} value in concentrations up to 100 μM

(Table 3, entry 4). Compound *rac*-**16gf**, which showed the highest affinity in the binding assays (pK_i = 6.67; Table 2, entry 11), also displayed the highest inhibitory potency of this series of hydrazones in the uptake assays at mGAT1 (pIC_{50} = 4.64; Table 3, entry 3). The observed subtype selectivities for the investigated compounds towards mGAT1 are considerably low and *rac*-**18fy** even showed its highest potency towards mGAT4 (pIC_{50} = 4.82; Table 3, entry 6).

Table 3. Comparison of inhibitory potencies (pIC_{50}) of best binders at mGAT1–mGAT4 from [^{3}H]GABA uptake experiments

		pIC_{50}[a]			
entry	compd	mGAT1	mGAT2	mGAT3	mGAT4
1	*rac*-**16e**	4.38±0.15	65%	59%	53%
2	*rac*-**16ga**	4.09±0.07	91%	57%	57%
3	*rac*-**16gf**	4.64±0.10	64%	4.48±0.09	4.12±0.08
4	*rac*-**16gg**	50%	84%	65%	79%
5	*rac*-**18e**	4.35±0.10	4.27±0.09	4.23±0.09	4.38±0.03
6	*rac*-**18fy**	4.45±0.10	4.27±0.03	4.59±0.09	4.82±0.012

[a]Results of [^{3}H]GABA uptake assays performed with HEK cells stably expressing mGAT1–mGAT4; pIC_{50} values are given as means±SEM of three independent experiments. In case of low inhibitory potencies percentages are given that represent remaining [^{3}H]GABA uptake in presence of 100 µM test compound.

The pIC_{50} values at mGAT1 from the uptake experiments are surprisingly low compared to the pK_i values from the binding experiments and the nominal differences of the values (pIC_{50} and pK_i) obtained in the two different test systems amounts to almost two log units. For comparison, for tiagabine (**5**) a pIC_{50} of 6.88±0.12 was established in [^{3}H]GABA uptake assays at mGAT1,[55] which is less than about 0.7 log units lower than its nominal pK_i value from the MS binding experiments. To verify this unexpected outcome, i.e. the large difference between the binding affinities (pK_i) and the inhibitory potencies (pIC_{50}) at mGAT1, we characterized GAT1 mediated GABA uptake also at hGAT1 (i.e. the human equivalent of this GABA transporter subtype). The results obtained from these experiments (see Supporting Information) were, however, essentially the same as those obtained in the [^{3}H]GABA uptake assays for mGAT1.

So far, several hundreds of derivatives of nipecotic acid (**2**), guvacine (**3**), and related heterocyclic amino acids functionalized at the nitrogen atom with lipophilic arylalkyl residues have been characterized in our group in binding and uptake assays.[34,39,40,51,52,56] For all these compounds, pK_i values (from binding assays) were observed that are typically higher than the pIC_{50} values (from uptake experiments) but no more than about one log unit. Possibly, this discrepancy is due to differences in experimental parameters of the two test systems such as the target material (i.e. whole cells versus membrane fragments), the buffer constituents or the incubation protocol. Furthermore, it is worth mentioning that this phenomenon was reported by others also for monoamine transporter inhibitors characterized in binding and uptake assays (e.g. at the serotonin transporter).[57] Hence, the disappointingly low inhibitory potencies of the synthesized hydrazones determined in mGAT1 uptake assays (pIC_{50}) as compared to the binding affinities (pK_i) were rather surprising. Even taking into account that there is a certain degree of uncertainty in the stated values, it could be concluded that this extent of discrepancy between affinity and inhibitory potency was remarkably higher than observed by us for other GAT1 inhibitors so far. A possible instability of the hydrazones in the “Krebs”

incubation buffer of the uptake experiments (containing glucose and Tris)[55] as explanation of this phenomenon could be ruled out by control experiments (see Supporting Information). Thus, the question arose if the synthesized hydrazones address the predicted binding site of known bench mark GAT1 inhibitors such as tiagabine (**5**) and NO711 (**6**).

Mode of interaction.

In order to shed light on the mode of interaction of the herein introduced hydrazones, *rac*-**16gf** (chosen as the most potent compound of the described series of hydrazones) and *rac*-**16gg** (chosen as the compound showing the highest difference between affinity in binding assays and inhibitory potency in uptake assays) were exemplarily examined, whether they inhibit the binding of NO711 (**6**) at mGAT1 in a competitive or non-competitive manner. For this purpose, saturation experiments with NO711 (**6**) at mGAT1 in the presence of fixed concentrations of *rac*-**16gf**, *rac*-**16gg** and tiagabine (**5**) were performed. The latter was applied as a GAT1 ligand generally assumed to inhibit NO711 (**6**) binding in a competitive way. Finally, the resulting saturation isotherms were

compared with those obtained in the absence of these compounds (for experimental details see experimental section).

In the presence of 100 nM and 1 μM tiagabine (**5**; the applied concentrations are about 0.6 and 1.6 log units higher than its corresponding pK_i value) the obtained saturation isotherms showed that the density of binding sites (B_{max}) for NO711 (**6**) remained unchanged whereas the "apparent" equilibrium dissociation constants (K_{d_app}) of **6** were significantly enhanced (see Figure 3 and Table 4). Both results are completely in line with a competitive inhibition of NO711 (**6**) binding by tiagabine (**5**). According to Hulme and Trevethick,[58] a competitive binding interaction in this kind of saturation experiment can also be proven with a Schild-like plot. In a Schild-like plot the logarithm of the term $\left(\frac{K_{d\_app}}{K_d} - 1\right)$, whereby K_{d_app} is the "apparent" K_d (in the presence of the test compound) and K_d is the "true" K_d (in the absence of test compounds), is displayed as a function of the concentration of the test compound. In the present case a slope (here for the sake of simplicity referred to as Schild-like coefficient, see Table 4) of 1.05±0.05 was found which

further demonstrates the competitive character of the interaction between tiagabine (**5**) and NO711 (**6**) at mGAT1.

The saturation isotherms obtained in presence of *rac*-**16gf** and *rac*-**16gg** in concentrations of 1 µM and 10 µM (i.e. concentrations about 0.6 and 1.7 log units higher than their corresponding pK_i values) were distinctly different as compared to those obtained in presence of tiagabine (**5**). Both compounds, *rac*-**16gf** and *rac*-**16gg**, led to a significant decrease of B_{max}, indicating a non-competitive interaction with respect to binding of NO711 (**6**) and the investigated hydrazones at mGAT1. The "apparent" K_d values in the presence of *rac*-**16gf** and *rac*-**16gg** are increased as well, but in this case in contrast to tiagabine (**5**) the calculated Schild-like coefficients amounted to only 0.49±0.10 and 0.57±0.12 for *rac*-**16gf** and *rac*-**16gg**, respectively (Table 4), arguing for a negative cooperativity according to Hulme and Trevethick.[58] Taken together, these results indicate that inhibition of NO711 (**6**) binding at mGAT1 by the investigated hydrazones *rac*-**16gf** and *rac*-**16gg** is non-competitive and possibly not due to binding at the same site addressed by the reporter ligand **6** as well as by tiagabine (**5**).

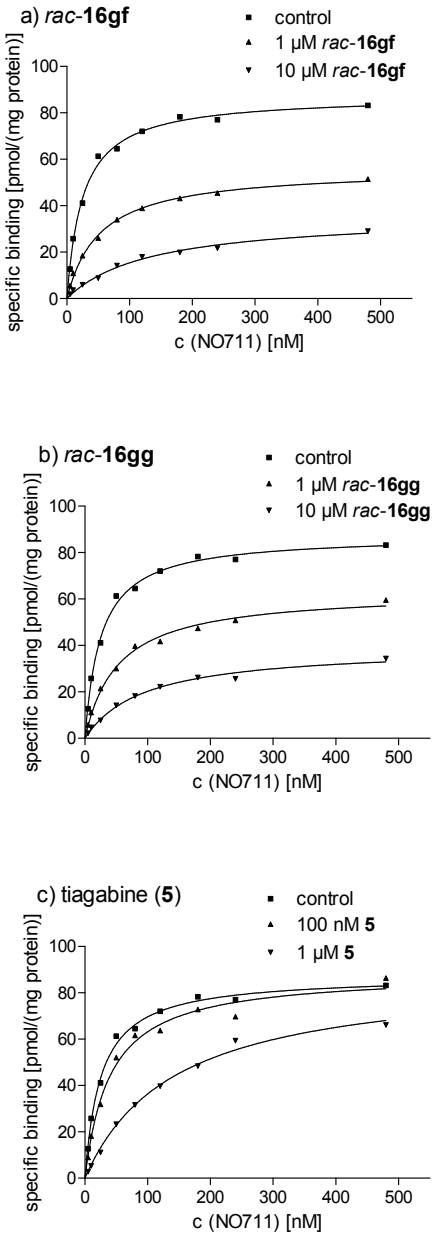

Figure 3. Saturation isotherms for NO711 (**6**) as reporter ligand addressing mGAT1. Data points represent specific binding (means from triplicates) obtained in the presence of a)

rac-**16gf**, b) *rac*-**16gg** and c) tiagabine (**5**) (in different fixed concentrations as indicated) and for control also in the absence of any additional test compound.

Table 4. Characterization of the mode of interaction between the reporter ligand (6) and compounds *rac*-16gf, *rac*-16gg and 5.[a]

compd	parameters	inhibitor[b] 100 nM	1 µM	10 µM	absent	coefficient[c]	conclusion
rac-**16gf**	B_{max} [pmol/mg]	-	48.4±3.9**	28.3±4.1**		0.49±0.10	non-competitive
	K_{d_app} [nM]	-	56.0±7.1	111.9±11.9*	-		
rac-**16gg**	B_{max} [pmol/mg]	-	57.1±3.6*	38.9±1.9**	-	0.57±0.12	non-competitive
	K_{d_app} [nM]	-	57.7±3.8**	154.2±45.9			
5	B_{max} [pmol/mg]	79.9±4.3	81.0±7.2	-	-	1.05±0.05	competitive
	K_{d_app} [nM]	40.5±1.0**	146.8±7.7**	-	-		
control	B_{max} [pmol/mg]	-	-	-	79.5±5.0	-	-
	K_d [nM]	-	-	-	28.3±1.5		

[a]Determined in saturation experiments using NO711 (**6**) as reporter ligand for mGAT1.

[b]Saturation experiments were performed in the presence and absence (control) of *rac*-

16gf, *rac*-**16gg** and **5** (in different fixed concentrations as indicated). [c]Schild-like coefficients calculated according to Hulme and Trevethick.[58] All results are presented as means±SEM from three independently performed experiments. Statistically significant differences from control values are indicated by asterisks (*P < 0.025; **P < 0.01; according to two-tailed Student's t-tests).

For the sake of clarity, it should be pointed out that the term "non-competitive" is used only phenomenologically, both in literature[59–62] and herein, to indicate that interactions of ligands with GAT1 give rise to altered saturation isotherms (with respect to GABA uptake and NO711 (**6**) binding experiments, respectively). Hence and as commonly accepted, the term "non-competitive" does not specify the underlying mechanism by which a ligand interacts with its target, in the present case mGAT1. For instance, non-competitive inhibition modes can be the result of an allosteric modulation or be caused by an irreversible binding or very slow dissociating orthosteric ligand.[63] To our knowledge, no studies have been published so far that experimentally verified the localization of an allosteric binding site at GAT1 (e.g. by site-directed mutagenesis experiments). In order

to rule out the aforementioned kinetic phenomena (i.e. inhibition by irreversibly binding or very slow dissociating orthosteric ligands) as cause for the non-competitive inhibition mode of the hydrazones under discussion, the inhibitory potencies (pIC_{50}) of these compounds were determined in additional GABA uptake experiments using different time periods for preincubation, i.e. in one set of experiments 0 min instead of the commonly applied 25 min. The experimental details as well as the results obtained thereby are included in the Supporting Information. In short, the inhibitory potencies of the six hydrazones, *rac*-**16e**, *rac*-**16ga**, *rac*-**16gf**, *rac*-**16gg**, *rac*-**18e**, *rac*-**18fy**, obtained when the preincubation time amounted to 0 min, are in a similar order of magnitude (i.e. pIC_{50} values in a range from 3.77 to 4.57) as those recorded for the previous experiments (i.e. with the preincubation time amounting to 25 min, pIC_{50} values in a range from 3.87 to 4.51 were obtained) with the nominal differences obtained for the two different incubation periods being minor and insignificant (nominal differences between 0 and 25 min preincubation amounting to only 0.1–0.4 log units). According to these results a kinetic phenomenon as explanation for the observed non-competitive behavior appears highly unlikely, thus supporting an allosteric mode of action at GAT1.

To gain insights in the functional consequences (i.e. regarding the inhibition of the GABA transport) associated with the non-competitive interaction of the hydrazones *rac*-**16gf** and *rac*-**16gg** with GAT1, further GABA uptake experiments were performed, in which either no inhibitor was applied, or hydrazones *rac*-**16gf** and *rac*-**16gg**, or finally tiagabine (**5**) as an example for a competitively acting compound. These experiments were carried out in form of MS based GABA uptake saturation experiments with ($^2H_6$)GABA as substrate using COS cells stably expressing hGAT1 as previously reported.[64,65] The saturation curves obtained from the saturation experiments in presence of the hydrazones *rac*-**16gf** and *rac*-**16gg** as well as tiagabine (**5**), which were applied in concentrations of about or below their pIC_{50} values, together with those from the control experiments (i.e. saturation curves obtained in the absence of GAT inhibitors) are exemplarily depicted in Figure 4. The K_m and K_{m_app} ("apparent" Michaelis-Menten constants in the presence of GAT inhibitors) as well as V_{max} values calculated from the data of these saturation experiments are shown in Table 5. As can be seen from these data, in presence of tiagabine (**5**) the maximum velocities for ($^2H_6$)GABA transport at hGAT1 (i.e. V_{max}) are slightly decreased while the "apparent" Michaelis-Menten constants (K_{m_app}) are distinctly increased (see

Table 5). The higher K_{m_app} values effected by tiagabine (**5**) are in line with a competitive inhibition mode, whereas the reduced V_{max} values are atypical for a competitive inhibitor, which is a result, however, that has already been reported before in literature for this compound (referred to as mixed competitive/non-competitive inhibition mode).[66] Given that tiagabine (**5**) is commonly considered to competitively address the substrate binding site at GAT1,[33,34] we assume that the slightly decreased V_{max} values are at least partly due to the experimental conditions of the uptake experiment (with a 25 min preincubation period for preequilibration of the test compound with the target). Conversely, the observed behavior of the hydrazones *rac*-**16gf** and *rac*-**16gg** appeared to be completely different: Both, the V_{max} values and the K_{m_app} values are substantially decreased (see Table 5), again indicating a non-competitive behavior of the hydrazones *rac*-**16gf** and *rac*-**16gg**, this time affecting the inhibition of the GABA transport at hGAT1 (while in the initial experiments described above a non-competitive inhibition of the NO711 (**6**) binding at mGAT1 was observed).

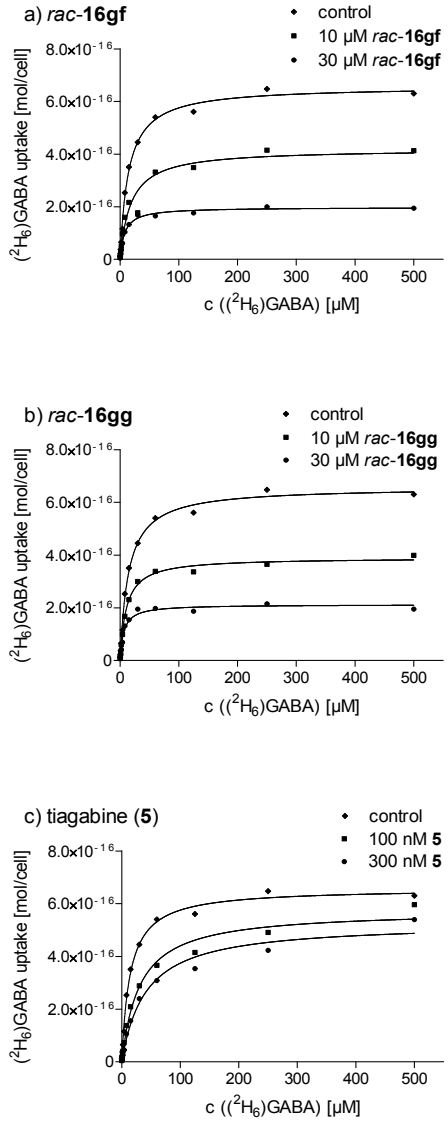

Figure 4. Saturation isotherms for the ($^2H_6$)GABA uptake at hGAT1. Data points represent specific uptake (means from triplicates) obtained in the presence of a) *rac*-**16gf**, b) *rac*-

16gg and c) tiagabine (5) (in different fixed concentrations as indicated) and for control (i.e. in the absence of any GAT inhibitor).

Table 5. Characterization of the mode of GABA uptake inhibition at GAT1 by compounds *rac*-16gf, *rac*-16gg and 5.[a]

compd	pIC_{50}[b] (hGAT1)	para-meters	inhibitor[c] 100 nM	300 nM	10 µM	30 µM	absent	conclusion
rac-16gf	4.37	V_{max}[d]	-	-	332±56**	165±27**	-	non-
	±0.06	K_{m_app}[d]	-	-	10.1±4.0	5.7±1.1**	-	competitive
rac-16gg	3.87	V_{max}[d]	-	-	341±26**	183±26**	-	non-
	±0.03	K_{m_app}[d]	-	-	8.2±1.2*	5.1±0.6**	-	competitive
5	6.81	V_{max}[d]	491±61*	419±59**	-	-	-	mixed[f]
	±0.15[e]	K_{m_app}[d]	19.7±5.5	29.4±5.8*	-	-	-	
control	-	V_{max}[d]	-	-	-	-	570±53	-
		K_m[d]	-	-	-	-	12.0±1.2	

[a]Determined in saturation experiments based on MS Transport Assays at hGAT1. [b]The inhibitory potencies (pIC_{50}) at hGAT1 were determined in competition experiments based on MS Transport Assays. [c]Saturation experiments were performed in the presence and

absence (control) of *rac*-**16gf**, *rac*-**16gg** and **5** (in different fixed concentrations as indicated). All results are presented as means±SEM from three independently performed experiments. [d]V_{max} values are given in [amol/cell • min], K_m values in [µM]. Statistically significant differences from control values are indicated by asterisks (*P < 0.05; **P < 0.01; according to paired, one-tailed Student's t-tests). [e]Value from reference.[64] [f]Mixed competitive/non-competitive, see discussions in the text.

Most notably, the herein introduced hydrazones lead to an increase of the affinity for the substrate GABA (**1**) towards its particular transporter, given the fact that the "apparent" Michaelis-Menten constants (K_{m_app}; see Table 5) for the GABA uptake at GAT1 are distinctly reduced in the presence of *rac*-**16gf** and *rac*-**16gg**. This observation, as well as the aforementioned results of the experiments using different incubation periods, clearly indicate an allosteric mode of action as explanation for the non-competitive interaction between the aforementioned hydrazones and GAT1.

As noted above molecular modeling had indicated that nipecotic acid derivatives with lipophilic residues attached to the 5-position via an appropriate spacer might represent a

new class of GAT1 inhibitors. Being designed for the binding region representing the putative binding site of competitive GAT1 inhibitors such as tiagabine (**5**) these compounds had to be expected to show the same mode of action, in other words to be competitive GAT1 inhibitors as well. Hence, it can be considered as a matter of serendipity that though the design aimed at competitive inhibitors, allosteric inhibitors most likely addressing a different binding site have been identified.

The distinct numerical differences observed between the pK_i values from the binding experiments and the pIC_{50} values from uptake experiments can hardly be explained by the allosteric mode of action of the hydrazone inhibitors alone. A conceivable explanation could be that binding of ligands or just different experimental conditions (including target material and buffer composition as already mentioned in the previous section) cause differences in the GAT1 conformation and the structure of the allosteric and the substrate binding site, which influence affinity and potency of investigated test compounds in the way observed in this study. Although such phenomena are well known for neurotransmitter receptors such as the nicotinic acetylcholine receptor,[67] they have not yet been reported for GABA transporters so far. Hence, further investigations are required

to elucidate this issue and also to improve the understanding of GAT1 mediated GABA transport in general.

The identified hydrazine inhibitors will be valuable tool compounds for mechanistic and pharmacological studies, though their pK_i and pIC_{50} values are lower than those for common competitive GAT1 inhibitors such as tiagabine (**5**), to which, however, they cannot be compared, as they address a different, namely, an allosteric instead of the competitive binding site (though it is generally desirable to have benchmark inhibitors as reference compounds in the assays used to characterize biological activities in a medicinal chemistry study – as we did with tiagabine herein).

Potential of the identified hydrazone hits allosterically interacting with GAT1.

Up to now, only few examples of non-competitive inhibitors of GAT1 are known, for most of which the mechanistic rationale (e.g. allosteric modulation or irreversible binding) for their non-competitive behaviors has still to be elucidated. Sarup et al.[59] described different N-substituted 3-hydroxy-4-amino-4,5,6,7-tetrahydro-1,2-benzisoxazols of which some,

such as compound **39** (see Chart 3; pIC_{50} 5.7 for inhibition of GABA uptake at mGAT1) were revealed as GAT1 inhibitors with non-competitive mode of inhibition (based on reduced V_{max} values in GABA uptake saturation experiments). A structurally related compound of **39**, referred to as EF1502 (**40**), was shown to inhibit both mGAT1 and mGAT2 (≙ BGT1 according to HUGO) non-competitively (pIC_{50} 5.4 at mGAT1 and pIC_{50} 4.7 at mGAT2, data refer to the more potent (*R*)-enantiomer of **40**).[60,61] Timple et al.[62] described the lignan derivative **41** as a non-competitive inhibitor of several neurotransmitter transporters of the SLC6 family including the dopamine and the norepinephrine transporters as well as GAT1 (pIC_{50} 4.7 at hGAT1). For the latter target an allosteric modulation of the GABA (**1**) transport was proposed (based on reduced V_{max} and K_{m_app} values in GABA uptake saturation experiments). Remarkably, none of the aforementioned non-competitive inhibitors, **39**–**41**, contains a free amino acid moiety let alone a nipecotic acid (**2**) subunit. Only compounds **39** and **40** can be considered to display a subunit analogous to an amino acid, by accounting the 3-hydroxyisoxazol moiety as a bioisosteric replacement for a carboxylic acid.[68,69] Still, the hydrazones

described herein represent a new class of allosteric GAT1 inhibitors differing substantially from the non-competitive inhibitors known so far.

Chart 3. Compounds proposed as non-competitive GAT1 inhibitors (39–41) in literature

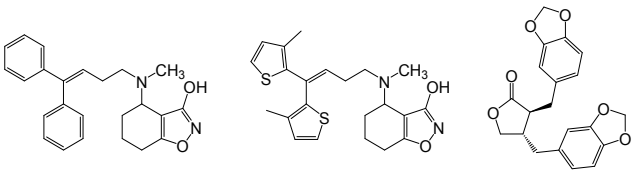

39 EF1502 (**40**) **41**

Interestingly, the (*R*)-enantiomer of EF1502 (**40**), despite being clearly less potent than tiagabine (**5**) at GAT1 *in vitro*, has already been shown to exhibit potent anticonvulsant effects in different *in vivo* models and, furthermore, to interact synergistically with tiagabine (**5**), while potential adverse effects were only additive.[61] Although the pharmacological profile of the hydrazones *rac*-**16gf** and *rac*-**16gg** is not sufficiently evaluated so far, it can be assumed that these compounds could also mediate promising pharmacological effects, as these compounds share several common features with EF1502 (**40**), i.e. they interact non-competitively at GAT1, address other GAT subtypes apart from GAT1 and have inhibitory potencies in a similar range. However, the herein

introduced hydrazones also display noteworthy differences in the biological activities as compared to EF1502 (**40**), making hydrazones *rac*-**16gf** and *rac*-**16gg** highly interesting complementary compounds. For instance, they exhibit a different profile of subtype selectivities: While EF1502 (**40**) inhibits both mGAT1 and mGAT2 (≙ BGT1) with similar potencies, hydrazones *rac*-**16gf** and *rac*-**16gg** are less potent at mGAT2, but show potencies at mGAT3 and mGAT4, respectively, almost as high as at mGAT1 (see Table 3). Furthermore, and possibly even more important, the capability of compounds *rac*-**16gf** and *rac*-**16gg** to increase the affinity for the substrate at GAT1 (i.e. reducing the "apparent" Michaelis-Menten constants; K_{m_app}) and at the same time to reduce the maximum velocity (V_{max}) of GABA transport provides a pharmacological potential that has not been explored up to date. To our knowledge, only the lignan derivative **41** has so far been reported to reduce the "apparent" Michaelis-Menten constants (K_{m_app}) for the substrate at GAT1 similarly as it is shown here for the hydrazones *rac*-**16gf** and *rac*-**16gg**. Conversely, this compound, **41**, was more active at dopamine and norepinephrine transporters than at GAT1 and was thus published in the context of a potential drug therapy for the attention deficit hyperactivity disorder.[62] Hydrazone *rac*-**16gf** is about

equally potent at GAT1 as lignan derivative **41** (with respect to the nominal pIC_{50} values) and in this context it is worth mentioning that the hydrazones are, in contrast to compound **41**, still racemic, therefore providing the possibility that the corresponding eutomers could be even slightly more potent.

Hence, the herein introduced 5-substituted nipecotic acid derivatives represent valuable new tools for investigation of allosteric modulation of GAT1 mediated GABA uptake *in vitro*. These compounds may also exert a promising new pharmacological profile by their specific mode of GAT inhibition and be a helpful starting point for the development of distinctly more affine and potent GAT1inhibitors addressing the allosteric binding site under discussion. Finally, based on experiences with analogous compounds,[51] it appears reasonable to assume that the hydrazone function within the spacer of this class of synthesized compounds can be replaced by a corresponding propenyl group, leading to stable carba analogs without remarkable loss of functional activity that should be well suitable for future *in vivo* experiments.

CONCLUSION

In summary, nipecotic acid derivatives with a novel substitution pattern were explored with the aim of finding new GABA uptake inhibitors. Therefore, the 5-substituted nipecotic acid derivatives *rac*-**11**–*rac*-**14** possessing a hydrazine function were synthesized and applied as building blocks in DCC reactions with appropriate aldehydes for the generation of pseudostatic hydrazone libraries, which were screened for their affinities towards mGAT1 by means of MS Binding Assays.[35,51] This approach, i.e. the combined generation and screening of pseudostatic hydrazone libraries by means of MS Binding Assays, was again found to represent a powerful tool for structure-activity relationship studies of ligands for mGAT1, and it finally revealed new lipophilic moieties for 5-substituted nipecotic acid derivatives as GAT1 ligands. A total of nearly 900 hydrazones could be screened towards mGAT1, of which the 16 most active were selected for further evaluation of their binding affinities. The six best binders, *rac*-**16e**, *rac*-**16ga**, *rac*-**16gf**, *rac*-**16gg**, *rac*-**18e** and *rac*-**18fy** with pK_i values of 6.21–6.67, are *cis*-configured with respect to the substituents of the piperidine ring and are characterized by 5-arylfuran-2-yl residues as lipophilic domains, a moiety that is not known so far in GABA uptake

inhibitors. With a pK_i value of 6.67 compound *rac*-**16gf** bearing a 5-(1-naphthyl)furan-2-yl residue and a four atom spacer showed the highest binding affinity within the series of hydrazones described in this study. Furthermore, the six best binders were subjected to functional characterization at the different GABA transporter subtypes, at which, however, they displayed rather low to moderate inhibitory potencies (pIC_{50} values up to 4.64 at mGAT1) and low subtype selectivities. In MS binding experiments with NO711 (**6**) as reporter ligand addressing mGAT1 and compound *rac*-**16gf** as well as *rac*-**16gg** a non-competitive mode of interaction between the binding of the evaluated hydrazones and the reporter ligand could be demonstrated. Additional uptake experiments furthermore suggested an allosteric mode of action of the GABA (**1**) transport at GAT1.

Hence, it can be concluded that substitution of the 5-position of nipecotic acid represents an interesting structural variation leading to new GAT1 inhibitors with an interaction mode that differs distinctly from that of well-known GAT1 inhibitors such as tiagabine (**5**). And, more notably, those hydrazones, which represent the first allosteric modulators of GAT1 derived from nipecotic acid (**2**), might emerge as valuable tools for investigations with the aim to gain more insights in the physiological relevance of allosteric modulation of GAT1.

EXPERIMENTAL SECTION

Chemistry. Solvents for synthesis, extraction and flash chromatography were distilled before use. Anhydrous THF was prepared by drying over benzophenone/Na. Other commercially available reagents (by ABCR, Acros, Alfa Aesar, Fisher Scientific, Maybridge, Merck, Sigma-Aldrich, TCI and VWR) were used without further purification. TLC was carried out on precoated silica gel F_{254} glass plates (Merck) and detected under UV-light (λ = 254 and 366 nm) or by staining with a ninhydrin solution (0.3 g ninhydrin and 3 mL acetic acid dissolved in 100 mL 1-butanol).[70] Flash column chromatography was performed on silica gel 60 (grading 0.035–0.070 mm, purchased from Merck and Acros). NMR spectroscopy was performed on Avance III HD Bruker BioSpin (Bruker; ^{1}H NMR: 400 or 500 MHz, ^{13}C NMR: 101 or 126 MHz, ^{19}F NMR: 376 MHz) or JNMR-GX (JEOL; ^{1}H NMR: 400 or 500 MHz, ^{13}C NMR: 101 or 126 MHz) spectrometers. The spectra were processed with the NMR software MestReNova, versions 8.1, 10.0 and 12.0 (Mestrelab Research S.L.). Chemical shifts were internally referenced to TMS or MeOH (for samples

dissolved in D_2O), except for hydrazones, which were referenced to DMSO solvent signals (^{1}H NMR: 2.53 ppm; ^{13}C NMR: 39.13 ppm). IR spectroscopy was performed on a FT-IR Paragon 1000 (Perkin-Elmer) spectrometer and analyzed with the software Spectrum v2.00 (Perkin-Elmer). Samples were either pressed in KBr pellets or prepared as films between NaCl plates. High-resolution mass spectrometry was performed with Jeol MStation sector field mass spectrometer (Jeol), Thermo Finnigan MAT 95 (ThermoFischer Scientific) (both EI) or Thermo Finnigan LTQ FT Ultra mass spectrometer (ThermoFischer Scientific) (ESI). Elemental analysis for hydrazines *rac*-**11**–*rac*-**14** was performed with a Vario Micro Cube or Vario EL Cube (Elementar) and an 888 Titrando (Metrohm) in order to determine the corresponding amounts of hydrogen chloride and water of hydration.[49] Melting points were determined in open capillaries on a BÜCHI 510 melting point apparatus and are uncorrected. For purity testing quantitative NMR spectroscopy (qNMR) was performed in accordance to the journal protocol[71,72] on a Avance III HD Bruker BioSpin (Bruker; ^{1}H NMR: 400 MHz) spectrometer. As internal calibrants (IC) dimethyl sulfone (TraceCERT® certified reference compound, Lot-No.: BCBH9813V, purity: 99.73%) or maleic acid (TraceCERT® certified reference compound,

Lot-No.: BCBM8127V, purity: 99.94%) purchased from Sigma-Aldrich were used. The purity was calculated with the NMR software MestReNova, versions 10.0 and 12.0 (Mestrelab Research S.L.). The newly synthesized aldehydes and hydrazines were ≥ 95% pure. The metastable hydrazones[54] were used without purity determination but were synthesized from ≥ 95% pure building blocks in 1:1 mixture and completeness of the reaction was monitored by NMR. All individually synthesized hydrazones were checked for PAINS[73] with ZINC (http://zinc15.docking.org/patterns/home/);[74] no potential PAINS liabilities were identified with this *in silico* tool.

General procedure for the simultaneous hydrolysis of ester and cleavage of Boc protecting groups (GP1). The corresponding hydrazine precursor (1.0 eq.) was suspended in a 1 M aqueous HCl (30 eq.; 30 mL/mmol) and the mixture was heated to 60 °C in a sealed high-pressure tube for 3 h. Then the reaction was cooled to rt, diluted with H_2O (15 mL) and washed with DCM (3 x 15 mL). The aqueous solution was freeze dried.

General procedure for the hydrolysis of enol ethers (GP2). The corresponding enol ether (1.0 eq.) was dissolved in THF (11 mL/mmol), cooled to 0 °C and a 2 M aqueous HCl (3.7

eq.) was added. The reaction was stirred at 0 °C for 2 h and at rt for further 5–7 h. Then the reaction was quenched with $NaHCO_3$ (4.6 eq.) and dissolved in H_2O (20 mL). *iso*-hexane (5 mL) was added, the phases were separated and the aqueous phase was further extracted with DCM (4 x 25 mL). The combined organic phases were dried over Na_2SO_4 and concentrated under reduced pressure. The crude product was purified by flash chromatography on silica gel (EtOAc/*iso*-hexane = 1:3).

General procedure for the reductive hydrazine formation (GP3). The corresponding aldehyde (1.0 eq.) and *tert*-butyl carbazate (1.6 eq.) were dissolved in MeOH (33 mL/mmol) under Ar and stirred at rt for 1 h. Then the mixture was cooled to 0 °C, AcOH (2.5 eq.) and subsequently $NaBH_3CN$ (4.0 eq., in portions) were added. It was stirred at 0 °C for 2 h and at rt for further 80 min. Then the mixture was concentrated under reduced pressure, quenched with an aqueous $NaHCO_3$ solution (20 mL) and extracted with DCM (5 x 20 mL). The combined organic phases were dried over Na_2SO_4 and concentrated under reduced pressure. The crude product was purified by flash chromatography on silica gel (EtOAc/*iso*-hexane = 1:1).

General procedure for the preparation of hydrazones (GP4). The reactions were performed in sealed 1.5 mL tubes under Ar. To 850 µL DMSO-d_6 a 200 mM stock solution of the corresponding hydrazine hydrochloride[49] in D_2O (50 µL; 1.0 eq.; 0.010 mmol), a 1 M solution of NaOD in D_2O (20 µL/2.0 eq./0.020 mmol for *rac*-**11** x HCl and 30 µL/3.0 eq./0.030 mmol for *rac*-**13** x HCl) and D_2O (30 or 20 µL) were added to reach a total volume of 950 µL. The reaction was started by the addition of a 200 mM stock solution of the appropriate aldehyde in DMSO-d_6 (50 µL; 1.0 eq.; 0.010 mmol). The mixture was sonicated for 5–15 min and stored at rt over night. All NMR and HRMS measurements as well as the MS Binding Assays and GABA uptake assays were performed using this 10 mM solution without further purification.[54] Analysis of the ^{1}H NMR spectra showed that the reaction equilibrium was to ≥ 96% on the side of the products (determined by integration of the remaining signal of the aldehyde proton) and the hydrazones existed to ≥ 83% as *E*-isomers.

***rac*-(3*R*,5*S*)-[5-(Hydrazinylmethyl)piperidine-3-carboxylic acid]–hydrogen chloride–water (1/2/1) (*rac*-11 x HCl).** *rac*-**32** (53 mg; 0.14 mmol) was dissolved in a 2 M etheric HCl (4.8 mL; 9.6 mmol). The solution was stirred under Ar at rt for 3 d. Then the mixture

was concentrated under reduced pressure, diluted with H_2O (15 mL) and washed with DCM (3 x 15 mL). The aqueous solution was freeze dried and *rac*-**11** x HCl was obtained as white solid (36 mg; 85%). Mp 130 °C (decomposition). ^{1}H NMR (500 MHz, 1 M NaOD in D_2O, 25 °C): δ 1.14 (q, *J* = 12.4 Hz, 1 H), 1.65–1.77 (m, 1 H), 2.02 (d, *J* = 12.8 Hz, 1 H), 2.14 (t, *J* = 11.9 Hz, 1 H), 2.32 (tt, *J* = 12.0/3.7 Hz, 1 H), 2.43 (t, *J* = 11.9 Hz, 1 H), 2.57 (dd, *J* = 11.9/6.8 Hz, 1 H), 2.60 (dd, *J* = 11.9/6.8 Hz, 1 H), 2.98 (dm, *J* = 12.0 Hz, 1 H), 3.11 (dm, *J* = 11.9 Hz, 1 H) ppm.[75] ^{13}C NMR (126 MHz, 1 M NaOD in D_2O, 25 °C): δ 32.9, 34.2, 45.9, 48.2, 49.1, 57.9, 183.7 ppm. IR (film): $\tilde{\nu}$ 3421, 2962, 2839, 2810, 1723, 1589 cm^{-1}. HRMS (ESI): $[M+H]^+$ calcd. for $C_7H_{16}N_3O_2$, 174.1237; found, 174.1236. Purity (qNMR: 1 M NaOD in D_2O, 25 °C, maleic acid; m_S = 6.951 mg, m_{IC} = 9.117 mg): 96%.

***rac*-(3*R*,5*R*)-[5-(Hydrazinylmethyl)piperidine-3-carboxylic acid]–hydrogen chloride–water (1/3/1) (*rac*-12 x HCl).** According to **GP1** with *rac*-**31** (85 mg; 0.22 mmol) and a 1 M aqueous HCl (6.6 mL; 6.6 mmol). *rac*-**12** x HCl was obtained as white solid (57 mg; 87%). Mp 135 °C (decomposition). ^{1}H NMR (400 MHz, 1 M NaOD in D_2O, 25 °C): δ 1.56–1.65 (m, 1 H), 1.74–1.85 (m, 1 H), 1.87–1.96 (m, 1 H), 2.41 (tt, *J* = 7.7/4.3 Hz, 1 H), 2.48 (dd, *J* = 13.1/6.8 Hz, 1 H), 2.66 (dd, *J* = 12.0/6.7 Hz, 1 H), 2.70 (dd, *J* = 12.0/7.4 Hz, 1 H),

2.75–2.92 (m, 3 H) ppm.[75] ^{13}C NMR (101 MHz, 1 M NaOD in D_2O, 25 °C): δ 30.9, 31.2, 41.2, 47.5, 48.0, 56.3, 183.7 ppm. IR (film): $\tilde{\nu}$ 3428, 2958, 2851, 2366, 1719, 1618, 1595, 1560 cm^{-1}. HRMS (ESI): $[M+H]^+$ calcd. for $C_7H_{16}N_3O_2$, 174.1237; found, 174.1241. Purity (qNMR: 1 M NaOD in D_2O, 25 °C, maleic acid; m_S = 6.166 mg, m_{IC} = 5.709 mg): 98%.

***rac*-(3*R*,5*R*)-[5-(2-Hydrazinylethyl)piperidine-3-carboxylic acid]–hydrogen chloride–water (1/3/1) (*rac*-13 x HCl).** According to **GP1** with *rac*-**37** (69 mg; 0.17 mmol) and 1 M aqueous HCl (5.3 mL; 5.3 mmol). *rac*-**13** x HCl was obtained as white solid (46 mg; 85%). Mp 145 °C (decomposition). ^{1}H NMR (500 MHz, 1 M NaOD in D_2O, 25 °C): δ 1.11 (q, *J* = 12.3 Hz, 1 H), 1.29–1.43 (m, 2 H), 1.44–1.55 (m, 1 H), 2.02 (d, *J* = 12.8 Hz, 1 H), 2.11 (t, *J* = 11.8 Hz, 1 H), 2.30 (tt, *J* = 12.0/3.7 Hz, 1 H), 2.42 (t, *J* = 11.9 Hz, 1 H), 2.73 (dd, *J* = 12.3/7.0 Hz, 1 H), 2.76 (dd, *J* = 12.1/6.8 Hz, 1 H), 2.94 (dm, *J* = 12.2 Hz, 1 H), 3.09 (dm, *J* = 12.2 Hz, 1 H) ppm.[75] ^{13}C NMR (126 MHz, 1 M NaOD in D_2O, 25 °C): δ 31.5, 33.9, 34.8, 46.2, 48.2, 50.9, 51.1, 184.0 ppm. IR (film): $\tilde{\nu}$ 3409, 2955, 2802, 2562, 2347, 1723, 1560 cm^{-1}. HRMS (ESI): $[M+H]^+$ calcd. for $C_8H_{18}N_3O_2$, 188.1394; found, 188.1393. Purity (qNMR: 1 M NaOD in D_2O, 25 °C, maleic acid; m_S = 11.26 mg, m_{IC} = 8.962 mg): ≥ 99%.

rac-(3_R_,5_S_)-[5-(2-Hydrazinylethyl)piperidine-3-carboxylic acid]–hydrogen chloride–water (1/3/1) (_rac_-14 x HCl). According to **GP1** with _rac_-**38** (154 mg; 0.384 mmol) and 1 M aqueous HCl (11.5 mL; 11.5 mmol). _rac_-**14** x HCl was obtained as white solid (101 mg; 83%). Mp 143 °C (decomposition). ^{1}H NMR (400 MHz, 1 M NaOD in D_2O, 25 °C): δ 1.37–1.53 (m, 2 H), 1.53–1.66 (m, 2 H), 1.86–1.97 (m, 1 H), 2.34–2.51 (m, 2 H), 2.68–2.82 (m, 4 H), 2.85 (dd, J = 13.1/6.4 Hz, 1 H) ppm.[75] ^{13}C NMR (101 MHz, 1 M NaOD in D_2O, 25 °C): δ 29.6, 31.0, 32.7, 41.3, 47.5, 49.7, 51.5, 184.0 ppm. IR (film): $\tilde{\nu}$ 3415, 2955, 2850, 2569, 1719, 1571 cm^{-1}. HRMS (EI, 70 eV): M^+ calcd. for $C_8H_{17}N_3O_2$, 187.1321; found, 187.1332. Purity (qNMR: 1 M NaOD in D_2O, 25 °C, maleic acid; m_S = 5.076 mg, m_{IC} = 7.986 mg): ≥ 99%.

rac-(3_R_,5_S_)-(5-{[(_E_)-2-({5-[2-Chloro-4-(trifluoromethyl)phenyl]furan-2-yl}methylidene)hydrazin-1-yl]methyl}piperidine-3-carboxylic acid)–sodium chloride (1/2) (_rac_-16e).[54] According to **GP4** with _rac_-**11** x HCl, 5-[2-chloro-4-(trifluoromethyl)phenyl]-2-furaldehyde (**15e**) and 1 M NaOD (20 µL) _rac_-**16e** was obtained quantitatively in solution. Besides the major _E_-isomer the _Z_-isomer is present in 8%. ^{1}H NMR (500 MHz, DMSO-d_6/D_2O = 9:1, 25 °C): δ 1.22 (q, J = 12.5 Hz, 1 H), 1.99–2.10 (m, 1 H), 2.13 (d, J = 13.5

Hz, 1 H), 2.44–2.60 (m, 2 H), 2.73 (t, *J* = 12.5 Hz, 1 H), 3.09 (dd, *J* = 13.5/6.7 Hz, 1 H), 3.14 (dd, *J* = 13.7/6.2 Hz, 1 H), 3.28 (dd, *J* = 12.5/4.2 Hz, 1H), 3.35 (dd, *J* = 12.5/4.0 Hz, 1 H), 6.67 (d, *J* = 3.7 Hz, 1 H), 7.41 (d, *J* = 3.7 Hz, 1 H), 7.56 (s, 1 H), 7.80 (dd, *J* = 8.5/1.9 Hz, 1 H), 7.92 (s, 1 H), 8.07 (d, *J* = 8.4 Hz, 1 H) ppm.[75,76] ^{13}C NMR (126 MHz, DMSO-d_6/D_2O = 9:1, 25 °C): δ 30.4, 32.7, 39.8, 45.2, 46.0, 50.6, 109.3, 115.5, 123.3 (q, J_{CF} = 272.7 Hz), 123.8, 124.4 (q, J_{CF} = 4.4 Hz), 127.7 (q, J_{CF} = 4.1 Hz), 127.9, 128.1 (q, J_{CF} = 32.8 Hz), 128.9, 131.6, 146.7, 152.7, 173.9 ppm.[76] ^{19}F {^{1}H} NMR (376 MHz, DMSO-d_6/D2O = 9:1, 25 °C): δ -61.1 ppm.[76] HRMS (ESI): $[M+H]^+$ calcd. for $C_{19}H_{20}N_3O_3ClF_3$, 430.1140; found, 430.1139.

***rac*-(3*R*,5*S*)-(5-{[(*E*)-2-[(3-phenoxyphenyl)methylidene]hydrazin-1-yl]methyl}piperidine-3-carboxylic acid)–sodium chloride (1/2) (*rac*-16r).**[54] According to **GP4** with *rac*-**11** x HCl, 3-phenoxybenzaldehyde (**15r**) and 1 M NaOD (20 µL) *rac*-**16r** was obtained quantitatively in solution. Besides the major *E*-isomer the *Z*-isomer is present in 3%. ^{1}H NMR (500 MHz, DMSO-d_6/D_2O = 9:1, 25 °C): δ 1.19 (q, *J* = 12.3 Hz, 1 H), 1.97–2.06 (m, 1 H), 2.10 (d, *J* = 13.6 Hz, 1 H), 2.40–2.59 (m, 2 H), 2.71 (t, *J* = 12.5 Hz, 1 H), 3.02 (dd, *J* = 13.4/7.0 Hz, 1 H), 3.07 (dd, *J* = 13.5/6.2 Hz, 1 H), 3.25 (dd, *J* = 12.3/3.9 Hz, 1H), 3.33 (dd, *J* = 12.6/4.1

Hz, 1 H), 6.87 (ddd, *J* = 8.2/2.5/1.1 Hz, 1 H), 6.98–7.04 (m, 2 H), 7.09–7.13 (m, 1 H), 7.16 (tt, *J* = 7.6/1.1 Hz, 1 H), 7.24 (dd, *J* = 7.9/0.9 Hz, 1 H), 7.35 (t, *J* = 7.9 Hz, 1 H), 7.39–7.44 (m, 2 H), 7.57 (s, 1 H) ppm.[75,76] ^{13}C NMR (126 MHz, DMSO-d_6/D2O = 9:1, 25 °C): δ 30.5, 32.8, 40.0, 45.2, 46.1, 50.9, 114.2, 117.6, 118.7, 120.7, 123.6, 130.2, 130.3, 133.6, 138.6, 156.6, 157.0, 174.0 ppm.[76] HRMS (ESI): $[M+H]^+$ calcd. for $C_{20}H_{24}N_3O_3$, 354.1812; found, 354.1811.

***rac*-(3*R*,5*S*)-(5-{[(*E*)-2-{[5-(2-Chlorophenyl)furan-2-yl]methylidene}hydrazin-1-yl]methyl}piperidine-3-carboxylic acid)–sodium chloride (1/2) (*rac*-16fv).**[54] According to **GP4** with *rac*-**11** x HCl, 5-(2-chlorophenyl)-2-furaldehyde (**15fv**) and 1 M NaOD (20 µL) *rac*-**16fv** was obtained quantitatively in solution. Besides the major *E*-isomer the *Z*-isomer is present in 9%. ^{1}H NMR (500 MHz, DMSO-d_6/D2O = 9:1, 25 °C): δ 1.21 (q, *J* = 12.5 Hz, 1 H), 2.02–2.09 (m, 1 H), 2.13 (d, *J* = 13.7 Hz, 1 H), 2.42–2.61 (m, 2 H), 2.73 (t, *J* = 12.5 Hz, 1 H), 3.07 (dd, *J* = 13.4/6.9 Hz, 1 H), 3.12 (dd, *J* = 13.5/6.2 Hz, 1 H), 3.28 (dd, *J* = 12.6/4.0 Hz, 1H), 3.34 (dd, *J* = 12.6/4.0 Hz, 1 H), 6.62 (d, *J* = 3.6 Hz, 1 H), 7.19 (d, *J* = 3.6 Hz, 1 H), 7.33 (td, *J* = 7.7/1.7 Hz, 1 H), 7.45 (td, *J* = 7.6/1.3 Hz, 1 H), 7.55 (dd, *J* = 7.2/1.0 Hz, 1 H), 7.56 (s, 1 H), 7.86 (dd, *J* = 8.0/1.7 Hz, 1 H) ppm.[75,76] ^{13}C NMR (126 MHz,

DMSO-d_6/D_2O = 9:1, 25 °C): δ 30.4, 32.7, 39.8, 45.1, 46.0, 50.8, 109.2, 113.2, 124.6, 127.5, 127.6, 128.1, 128.7, 128.7, 130.8, 148.1, 151.5, 173.9 ppm.[76] HRMS (ESI): $[M+H]^+$ calcd. for $C_{18}H_{21}N_3O_3Cl$, 362.1266; found, 362.1265.

***rac*-(3*R*,5*S*)-(5-{[(*E*)-2-{[5-(3-Chlorophenyl)furan-2-yl]methylidene}hydrazin-1-yl]methyl}piperidine-3-carboxylic acid)–sodium chloride (1/2) (*rac*-16fw).**[54] According to **GP4** with *rac*-**11** x HCl, 5-(3-chlorophenyl)-2-furaldehyde (**15fw**) and 1 M NaOD (20 µL) *rac*-**16fw** was obtained quantitatively in solution. Besides the major *E*-isomer the *Z*-isomer is present in 9%. ^{1}H NMR (500 MHz, DMSO-d_6/D_2O = 9:1, 25 °C): δ 1.22 (q, *J* = 12.5 Hz, 1 H), 1.99–2.09 (m, 1 H), 2.13 (d, *J* = 13.6 Hz, 1 H), 2.44–2.59 (m, 2 H), 2.74 (t, *J* = 12.5 Hz, 1 H), 3.07 (dd, *J* = 13.5/6.9 Hz, 1 H), 3.12 (dd, *J* = 13.6/6.4 Hz, 1 H), 3.28 (dd, *J* = 12.7/3.8 Hz, 1H), 3.35 (dd, *J* = 12.6/4.0 Hz, 1 H), 6.58 (d, *J* = 3.5 Hz, 1 H), 7.09 (d, *J* = 3.6 Hz, 1 H), 7.33 (dd, *J* = 8.1/2.1 Hz, 1 H), 7.45 (t, *J* = 7.9 Hz, 1 H), 7.55 (s, 1 H), 7.66 (dt, *J* = 8.0/1.2 Hz, 1 H), 7.74 (t, *J* = 1.9 Hz, 1 H) ppm.[75,76] ^{13}C NMR (126 MHz, DMSO-d_6/D_2O = 9:1, 25 °C): δ 30.4, 32.7, 39.8, 45.1, 46.0, 50.8, 109.4, 109.7, 121.8, 122.7, 124.9, 127.1, 131.0, 132.0, 133.8, 150.4, 151.9, 173.9 ppm.[76] HRMS (ESI): $[M+H]^+$ calcd. for $C_{18}H_{21}N_3O_3Cl$, 362.1266; found, 362.1265.

rac-(3*R*,5*S*)-(5-{[(*E*)-2-{[5-(2,4-Dichlorophenyl)furan-2-yl]methylidene}hydrazin-1-yl]methyl}piperidine-3-carboxylic acid)–sodium chloride (1/2) (*rac*-**16fy**).[54] According to **GP4** with *rac*-**11** x HCl, 5-(2,4-dichlorophenyl)-2-furaldehyde (**15fy**) and 1 M NaOD (20 µL) *rac*-**16fy** was obtained quantitatively in solution. Besides the major *E*-isomer the *Z*-isomer is present in 9%. ^{1}H NMR (500 MHz, DMSO-d_6/D_2O = 9:1, 25 °C): δ 1.23 (q, *J* = 12.5 Hz, 1 H), 1.99–2.10 (m, 1 H), 2.14 (d, *J* = 13.3 Hz, 1 H), 2.45–2.61 (m, 2 H), 2.75 (t, *J* = 12.4 Hz, 1 H), 3.08 (dd, *J* = 13.5/6.7 Hz, 1 H), 3.12 (dd, *J* = 13.6/6.3 Hz, 1 H), 3.28 (dd, *J* = 12.4/3.9 Hz, 1H), 3.36 (dd, *J* = 12.6/4.0 Hz, 1 H), 6.63 (d, *J* = 3.6 Hz, 1 H), 7.23 (d, *J* = 3.6 Hz, 1 H), 7.53 (dd, *J* = 8.6/2.2 Hz, 1 H), 7.55 (s, 1 H), 7.70 (d, *J* = 2.2 Hz, 1 H), 7.87 (d, *J* = 8.6 Hz, 1 H) ppm.[75,76] ^{13}C NMR (126 MHz, DMSO-d_6/D_2O = 9:1, 25 °C): δ 30.3, 32.7, 39.8, 44.9, 46.0, 50.7, 109.3, 113.7, 124.3, 127.1, 127.9, 128.6, 129.5, 130.2, 132.1, 147.2, 151.8, 173.7 ppm.[76] HRMS (ESI): $[M+H]^+$ calcd. for $C_{18}H_{20}N_3O_3Cl_2$, 396.0876; found, 396.0875.

rac-(3*R*,5*S*)-(5-{[(*E*)-2-({5-[2-(Trifluoromethyl)phenyl]furan-2-yl}methylidene)hydrazin-1-yl]methyl}piperidine-3-carboxylic acid)–sodium chloride (1/2) (*rac*-**16fz**).[54] According to **GP4** with *rac*-**11** x HCl, 5-[2-(trifluoromethyl)phenyl]-2-furaldehyde (**15fz**) and 1 M NaOD

(20 µL) *rac*-**16fz** was obtained quantitatively in solution. Besides the major *E*-isomer the *Z*-isomer is present in 12%. ^{1}H NMR (500 MHz, DMSO-d_6/D_2O = 9:1, 25 °C): δ 1.21 (q, *J* = 12.5 Hz, 1 H), 1.97–2.08 (m, 1 H), 2.12 (d, *J* = 13.6 Hz, 1 H), 2.43–2.59 (m, 2 H), 2.73 (t, *J* = 12.5 Hz, 1 H), 3.05 (dd, *J* = 13.4/6.9 Hz, 1 H), 3.10 (dd, *J* = 13.5/6.1 Hz, 1 H), 3.27 (dd, *J* = 12.6/3.9 Hz, 1H), 3.34 (dd, *J* = 12.5/4.1 Hz, 1 H), 6.61 (d, *J* = 3.5 Hz, 1 H), 6.83 (d, *J* = 3.5 Hz, 1 H), 7.54 (s, 1 H), 7.58 (t, *J* = 7.7 Hz, 1 H), 7.75 (t, *J* = 7.7 Hz, 1 H), 7.82 (d, *J* = 7.8 Hz, 1 H), 7.85 (d, *J* = 7.9 Hz, 1 H) ppm.[75,76] ^{13}C NMR (126 MHz, DMSO-d_6/D_2O = 9:1, 25 °C): δ 30.4, 32.8, 39.8, 45.0, 46.0, 50.8, 108.8, 112.3, 124.0 (q, J_{CF} = 273.4 Hz), 124.6, 124.7 (q, J_{CF} = 30.6 Hz), 126.8 (q, J_{CF} = 5.9 Hz), 128.5, 128.6 (q, J_{CF} = 1.7 Hz), 129.8, 132.8, 158.6, 152.5, 173.8 ppm.[76] ^{19}F {^{1}H} NMR (376 MHz, DMSO-d_6/D_2O = 9:1, 25 °C): δ -58.4 ppm.[76] HRMS (ESI): $[M+H]^+$ calcd. for $C_{19}H_{21}N_3O_3F_3$, 396.1530; found, 396.1528.

***rac*-(3*R*,5*S*)-(5-{[(*E*)-2-({5-[2-Chloro-5-(trifluoromethyl)phenyl]furan-2-yl}methylidene)hydrazin-1-yl]methyl}piperidine-3-carboxylic acid)–sodium chloride (1/2) (*rac*-16ga).[54]** According to **GP4** with *rac*-**11** x HCl, 5-[2-chloro-5-(trifluoromethyl)phenyl]-2-furaldehyde (**15ga**) and 1 M NaOD (20 µL) *rac*-**16ga** was obtained quantitatively in

solution. Besides the major *E*-isomer the *Z*-isomer is present in 8%. ^{1}H NMR (500 MHz, DMSO-d_6/D_2O = 9:1, 25 °C): δ 1.17 (q, *J* = 12.5 Hz, 1 H), 1.95–2.08 (m, 1 H), 2.12 (d, *J* = 13.1 Hz, 1 H), 2.30–2.42 (m, 1 H), 2.45–2.59 (m, 1 H), 2.67 (t, *J* = 12.5 Hz, 1 H), 3.08 (dd, *J* = 12.4/5.9 Hz, 1 H), 3.12 (dd, *J* = 12.7/5.3 Hz, 1 H), 3.25 (dd, *J* = 12.1/2.5 Hz, 1H), 3.31 (dd, *J* = 12.7/4.0 Hz, 1 H), 6.66 (d, *J* = 3.6 Hz, 1 H), 7.36 (d, *J* = 3.6 Hz, 1 H), 7.55 (s, 1 H), 7.65 (dd, *J* = 8.4/2.3 Hz, 1 H), 7.80 (d, *J* = 8.4 Hz, 1 H), 8.13 (d, *J* = 2.3 Hz, 1 H) ppm.[75,76] ^{13}C NMR (126 MHz, DMSO-d_6/D_2O = 9:1, 25 °C): δ 31.0, 32.7, 40.9, 45.9, 46.2, 50.5, 109.1, 114.8, 123.5 (q, J_{CF} = 4.0 Hz), 123.5, 123.7 (q, J_{CF} = 272.5 Hz), 124.6 (q, J_{CF} = 3.9 Hz), 128.4 (q, J_{CF} = 32.5 Hz), 129.0, 132.2, 132.5, 146.4, 152.5, 173.4 ppm.[76] ^{19}F {^{1}H} NMR (376 MHz, DMSO-d_6/D_2O = 9:1, 25 °C): δ -61.3 ppm.[76] HRMS (ESI): $[M+H]^+$ calcd. for $C_{19}H_{20}N_3O_3ClF_3$, 430.1140; found, 430.1139.

rac-(3*R*,5*S*)-(5-{[(*E*)-2-{[5-(4-Chloro-2-nitrophenyl)furan-2-yl]methylidene}hydrazin-1-yl]methyl}piperidine-3-carboxylic acid)–sodium chloride (1/2) (*rac*-16gb).[54] According to **GP4** with *rac*-**11** x HCl, 5-(4-chloro-2-nitrophenyl)-2-furaldehyde (**15gb**) and 1 M NaOD (20 µL) *rac*-**16gb** was obtained quantitatively in solution. Besides the major *E*-isomer the *Z*-isomer is present in 13%. ^{1}H NMR (500 MHz, DMSO-d_6/D_2O = 9:1, 25 °C): δ 1.20 (q, *J*

= 12.6 Hz, 1 H), 1.98–2.07 (m, 1 H), 2.11 (d, *J* = 13.3 Hz, 1 H), 2.41–2.60 (m, 2 H), 2.71 (t, *J* = 12.4 Hz, 1 H), 3.04 (dd, *J* = 13.5/6.9 Hz, 1 H), 3.09 (dd, *J* = 13.5/6.1 Hz, 1 H), 3.26 (dd, *J* = 13.1/3.8 Hz, 1H), 3.33 (dd, *J* = 12.6/4.2 Hz, 1 H), 6.60 (d, *J* = 3.6 Hz, 1 H), 6.93 (d, *J* = 3.5 Hz, 1 H), 7.44 (s, 1 H), 7.78 (dd, *J* = 8.6/2.1 Hz, 1 H), 7.86 (d, *J* = 8.5 Hz, 1 H), 8.05 (d, *J* = 2.1 Hz, 1 H) ppm.[75,76] ^{13}C NMR (126 MHz, DMSO-d_6/D_2O = 9:1, 25 °C): δ 30.5, 32.7, 40.0, 45.3, 46.1, 50.6, 108.8, 112.7, 121.3, 123.5, 123.8, 129.7, 132.4, 132.5, 145.5, 146.6, 153.6, 174.0 ppm.[76] HRMS (ESI): $[M+H]^+$ calcd. for $C_{18}H_{20}N_4O_5Cl$, 407.1117; found, 407.1117.

***rac*-(3*R*,5*S*)-(5-{[(*E*)-2-({5-[3-(Trifluoromethyl)phenyl]furan-2-yl}methylidene)hydrazin-1-yl]methyl}piperidine-3-carboxylic acid)–sodium chloride (1/2) (*rac*-16gc).**[54] According to **GP4** with *rac*-**11** x HCl, 5-[3-(trifluoromethyl)phenyl]-2-furaldehyde (**15gc**) and 1 M NaOD (20 µL) *rac*-**16gc** was obtained quantitatively in solution. Besides the major *E*-isomer the *Z*-isomer is present in 7%. ^{1}H NMR (500 MHz, DMSO-d_6/D_2O = 9:1, 25 °C): δ 1.21 (q, *J* = 12.5 Hz, 1 H), 2.00–2.09 (m, 1 H), 2.13 (d, *J* = 13.2 Hz, 1 H), 2.43–2.60 (m, 2 H), 2.73 (t, *J* = 12.5 Hz, 1 H), 3.08 (dd, *J* = 13.5/6.8 Hz, 1 H), 3.12 (dd, *J* = 13.6/6.4 Hz, 1 H), 3.28 (dd, *J* = 12.6/3.9 Hz, 1H), 3.35 (dd, *J* = 12.6/4.0 Hz, 1 H), 6.60 (d, *J* = 3.5 Hz, 1 H), 7.19

(d, J = 3.5 Hz, 1 H), 7.56 (s, 1 H), 7.62 (d, J = 7.9 Hz, 1 H), 7.67 (t, J = 8.0 Hz, 1 H), 7.99 (s, 1 H), 8.00 (d, J = 6.6 Hz, 1 H) ppm.[75,76] ^{13}C NMR (126 MHz, DMSO-d_6/D_2O = 9:1, 25 °C): δ 30.5, 32.7, 39.9, 45.2, 46.0, 50.7, 109.7, 109.7, 119.4 (q, J_{CF} = 3.8 Hz), 123.7 (q, J_{CF} = 4.0 Hz), 124.1 (q, J_{CF} = 273.5 Hz), 124.7, 127.0, 129.9 (q, J_{CF} = 32.0 Hz), 130.2, 131.0, 150.4, 152.1, 174.0 ppm.[76] ^{19}F {^{1}H} NMR (376 MHz, DMSO-d_6/D_2O = 9:1, 25 °C): δ -61.3 ppm.[76] HRMS (ESI): $[M+H]^+$ calcd. for $C_{19}H_{21}N_3O_3F_3$, 396.1530; found, 396.1528.

***rac*-(3*R*,5*S*)-(5-{[(*E*)-2-({5-[4-Fluoro-3-(trifluoromethyl)phenyl]furan-2-yl}methylidene)hydrazin-1-yl]methyl}piperidine-3-carboxylic acid)–sodium chloride (1/2) (*rac*-16ge).[54]** According to **GP4** with *rac*-**11** x HCl, 5-[4-fluoro-3-(trifluoromethyl)phenyl]-2-furaldehyde (**15ge**) and 1 M NaOD (20 µL) *rac*-**16ge** was obtained quantitatively in solution. Besides the major *E*-isomer the *Z*-isomer is present in 9%. ^{1}H NMR (500 MHz, DMSO-d_6/D_2O = 9:1, 25 °C): δ 1.22 (q, J = 12.5 Hz, 1 H), 1.99–2.11 (m, 1 H), 2.13 (d, J = 13.6 Hz, 1 H), 2.44–2.60 (m, 2 H), 2.74 (t, J = 12.5 Hz, 1 H), 3.07 (dd, J = 13.5/6.9 Hz, 1 H), 3.12 (dd, J = 13.5/6.3 Hz, 1 H), 3.28 (dd, J = 12.4/2.8 Hz, 1H), 3.35 (dd, J = 12.6/4.0 Hz, 1 H), 6.59 (d, J = 3.5 Hz, 1 H), 7.14 (d, J = 3.5 Hz, 1 H), 7.52–7.58 (m, 2 H), 7.99–8.07 (m, 2 H) ppm.[75,76] ^{13}C NMR (126 MHz, DMSO-d_6/D_2O = 9:1, 25 °C): δ 30.4, 32.7, 39.8,

45.1, 46.0, 50.7, 109.5, 109.8, 117.4 (qd, J_{CF} = 32.1/13.3 Hz), 118.2 (d, J_{CF} = 21.8 Hz), 121.6 (q, J_{CF} = 4.4 Hz), 122.5 (q, J_{CF} = 274.3 Hz), 124.8, 127.3 (d, J_{CF} = 3.7 Hz), 129.7 (d, J_{CF} = 8.7 Hz), 149.7, 152.0, 157.8 (dq, J_{CF} = 253.9/1.6 Hz), 173.9 ppm.[76] ^{19}F {^{1}H} NMR (376 MHz, DMSO-d_6/D_2O = 9:1, 25 °C): δ -117.65 (q, J_{FF} = 12.5 Hz), -60.14 (d, J_{FF} = 12.4 Hz) ppm.[76] HRMS (ESI): $[M+H]^+$ calcd. for $C_{19}H_{20}N_3O_3F_4$, 414.1435; found, 414.1434.

***rac*-(3*R*,5*S*)-(5-{[(*E*)-2-{[5-(naphthalen-1-yl)furan-2-yl]methylidene}hydrazin-1-yl]methyl}piperidine-3-carboxylic acid)–sodium chloride (1/2) (*rac*-16gf).[54]** According to **GP4** with *rac*-**11** x HCl, 5-(naphthalen-1-yl)-2-furaldehyde (**15gf**) and 1 M NaOD (20 µL) *rac*-**16gf** was obtained quantitatively in solution. Besides the major *E*-isomer the *Z*-isomer is present in 12%. ^{1}H NMR (500 MHz, DMSO-d_6/D_2O = 9:1, 25 °C): δ 1.23 (q, *J* = 12.5 Hz, 1 H), 2.02–2.11 (m, 1 H), 2.14 (d, *J* = 13.4 Hz, 1 H), 2.46–2.61 (m, 2 H), 2.75 (t, *J* = 12.5 Hz, 1 H), 3.07 (dd, *J* = 13.4/6.8 Hz, 1 H), 3.12 (dd, *J* = 13.5/6.2 Hz, 1 H), 3.29 (dd, *J* = 12.7/3.5 Hz, 1H), 3.36 (dd, *J* = 12.4/4.0 Hz, 1 H), 6.69 (d, *J* = 3.5 Hz, 1 H), 6.98 (d, *J* = 3.5 Hz, 1 H), 7.56–7.65 (m, 4 H), 7.80 (dd, *J* = 7.3/1.3 Hz, 1 H), 7.95 (d, *J* = 8.2 Hz, 1 H), 8.01 (dd, *J* = 7.9/1.7 Hz, 1 H), 8.42 (dd, *J* = 8.6/1.3 Hz, 1 H) ppm.[75,76] ^{13}C NMR (126 MHz, DMSO-d_6/D_2O = 9:1, 25 °C): δ 30.4, 32.8, 39.8, 45.1, 46.0, 50.9, 109.4, 111.7, 124.9,

125.3, 125.7, 125.7, 126.3, 127.1, 127.4, 128.6, 128.7, 129.2, 133.7, 151.6, 151.7, 173.8 ppm.[76] HRMS (ESI): $[M+H]^+$ calcd. for $C_{22}H_{24}N_3O_3$, 378.1812; found, 378.1811.

***rac*-(3*R*,5*S*)-(5-{[(*E*)-2-({5-[3,5-Bis(trifluoromethyl)phenyl]furan-2-yl}methylidene)hydrazin-1-yl]methyl}piperidine-3-carboxylic acid)–sodium chloride (1/2) (*rac*-16gg).**[54] According to **GP4** with *rac*-**11** x HCl, 5-[3,5-bis(trifluoromethyl)phenyl]-2-furaldehyde (**15gg**) and 1 M NaOD (20 µL) *rac*-**16gg** was obtained quantitatively in solution. Besides the major *E*-isomer the *Z*-isomer is present in 9%. ^{1}H NMR (500 MHz, DMSO-d_6/D_2O = 9:1, 25 °C): δ 1.22 (q, J = 12.6 Hz, 1 H), 2.02–2.10 (m, 1 H), 2.14 (d, J = 13.3 Hz, 1 H), 2.41–2.63 (m, 2 H), 2.73 (t, J = 12.5 Hz, 1 H), 3.10 (dd, J = 11.9/5.2 Hz, 1 H), 3.14 (dd, J = 11.9/4.8 Hz, 1 H), 3.28 (dd, J = 12.2/3.7 Hz, 1H), 3.35 (dd, J = 12.5/3.9 Hz, 1 H), 6.64 (d, J = 3.6 Hz, 1 H), 7.42 (d, J = 3.6 Hz, 1 H), 7.56 (s, 1 H), 7.94 (s, 1 H), 8.30 (s, 2 H) ppm.[75,76] ^{13}C NMR (126 MHz, DMSO-d_6/D_2O = 9:1, 25 °C): δ 30.3, 32.5, 39.8, 45.1, 45.9, 50.5, 109.6, 111.7, 119.9 (q, J_{CF} = 3.8 Hz), 123.2 (q, J_{CF} = 3.5 Hz), 123.2 (q, J_{CF} = 273.1 Hz), 123.9, 131.1 (q, J_{CF} = 33.0 Hz), 132.3, 148.8, 153.0, 173.8 ppm.[76] ^{19}F {^{1}H} NMR (376 MHz, DMSO-d_6/D_2O = 9:1, 25 °C): δ -61.6 ppm.[76] HRMS (ESI): $[M+H]^+$ calcd. for $C_{20}H_{20}N_3O_3F_6$, 464.1403; found, 464.1403.

rac-(3*R*,5*S*)-(5-{[(*E*)-2-{[5-(2-Bromophenyl)furan-2-yl]methylidene}hydrazin-1-yl]methyl}piperidine-3-carboxylic acid)–sodium chloride (1/2) (*rac*-**16gk**).[54] According to **GP4** with *rac*-**11** x HCl, 5-(2-bromophenyl)-2-furaldehyde (**15gk**) and 1 M NaOD (20 µL) *rac*-**16gk** was obtained quantitatively in solution. Besides the major *E*-isomer the *Z*-isomer is present in 9%. ^{1}H NMR (500 MHz, DMSO-d_6/D_2O = 9:1, 25 °C): δ 1.22 (q, *J* = 12.5 Hz, 1 H), 2.00–2.10 (m, 1 H), 2.13 (d, *J* = 13.4 Hz, 1 H), 2.41–2.60 (m, 2 H), 2.74 (t, *J* = 12.5 Hz, 1 H), 3.07 (dd, *J* = 13.4/6.8 Hz, 1 H), 3.11 (dd, *J* = 13.5/6.2 Hz, 1 H), 3.28 (dd, *J* = 12.6/3.9 Hz, 1H), 3.35 (dd, *J* = 12.5/4.1 Hz, 1 H), 6.62 (d, *J* = 3.6 Hz, 1 H), 7.22 (d, *J* = 3.5 Hz, 1 H), 7.26 (td, *J* = 7.7/1.7 Hz, 1 H), 7.49 (td, *J* = 7.6/1.4 Hz, 1 H), 7.56 (s, 1 H), 7.73 (dd, *J* = 8.1/1.3 Hz, 1 H), 7.80 (dd, *J* = 7.9/1.7 Hz, 1 H) ppm.[75,76] ^{13}C NMR (126 MHz, DMSO-d_6/D_2O = 9:1, 25 °C): δ 30.4, 32.8, 39.8, 45.1, 46.0, 50.8, 109.0, 112.8, 118.6, 124.7, 128.1, 128.5, 129.2, 130.2, 134.2, 149.3, 151.6, 173.9 ppm.[76] HRMS (ESI): $[M+H]^+$ calcd. for $C_{18}H_{21}N_3O_3Br$, 406.0761; found, 406.0761.

rac-(3*R*,5*S*)-(5-{[(*E*)-2-{[2-(naphthalen-2-yl)pyrimidin-5-yl]methylidene}hydrazin-1-yl]methyl}piperidine-3-carboxylic acid)–sodium chloride (1/2) (*rac*-**16ho**).[54] According to **GP4** with *rac*-**11** x HCl, 2-(naphthalen-2-yl)pyrimidine-5-carboxaldehyde (**15ho**) and 1 M

NaOD (20 µL) *rac*-**16ho** was obtained quantitatively in solution. Besides the major *E*-isomer the *Z*-isomer is present in 9%. ^{1}H NMR (500 MHz, DMSO-d_6/D_2O = 9:1, 25 °C): δ 1.27 (q, *J* = 12.8 Hz, 1 H), 2.06–2.22 (m, 2 H), 2.43–2.64 (m, 2 H), 2.76 (t, *J* = 12.4 Hz, 1 H), 3.16 (dd, *J* = 13.5/6.8 Hz, 1 H), 3.20 (dd, *J* = 13.6/6.0 Hz, 1 H), 3.32 (dd, *J* = 12.5/4.2 Hz, 1H), 3.37 (dd, *J* = 12.5/4.0 Hz, 1 H), 7.56–7.65 (m, 3 H), 7.96–8.00 (m, 1 H), 8.05 (d, *J* = 8.7 Hz, 1 H), 8.07–8.12 (m, 1 H), 8.48 (dd, *J* = 8.7/1.7 Hz, 1 H), 8.95 (s, 1 H), 9.00 (s, 2 H) ppm.[75,76] ^{13}C NMR (126 MHz, DMSO-d_6/D_2O = 9:1, 25 °C): δ 30.3, 32.7, 39.8, 45.0, 46.0, 50.5, 124.5, 126.8, 127.0, 127.5, 127.5, 127.7, 128.4, 128.5, 129.0, 132.8, 134.0, 134.4, 153.4, 161.0, 173.7 ppm.[76] HRMS (ESI): $[M+H]^+$ calcd. for $C_{22}H_{24}N_5O_2$, 390.1925; found, 390.1923.

***rac*-(3*R*,5*R*)-(5-{2-[(*E*)-2-({5-[2-Chloro-4-(trifluoromethyl)phenyl]furan-2-yl}methylidene)hydrazin-1-yl]ethyl}piperidine-3-carboxylic acid)–sodium chloride (1/3) (*rac*-18e).[54]** According to **GP4** with *rac*-**13** x HCl, 5-[2-chloro-4-(trifluoromethyl)phenyl]-2-furaldehyde (**15e**) and 1 M NaOD (30 µL) *rac*-**18e** was obtained quantitatively in solution. Besides the major *E*-isomer the *Z*-isomer is present in 17%. ^{1}H NMR (500 MHz, DMSO-d_6/D_2O = 9:1, 25 °C): δ 1.10 (q, *J* = 12.5 Hz, 1 H), 1.45–1.60 (m, 2 H), 1.73–1.85 (m, 1

H), 2.11 (d, *J* = 13.3 Hz, 1 H), 2.30 (tt, *J* = 12.6/3.8 Hz, 1 H), 2.43 (t, *J* = 12.2 Hz, 1 H), 2.65 (t, *J* = 12.4 Hz, 1 H), 3.14–3.20 (m, 3 H), 3.28 (dd, *J* = 12.2/3.6 Hz, 1 H), 6.65 (d, *J* = 3.6 Hz, 1 H), 7.40 (d, *J* = 3.6 Hz, 1 H), 7.50 (s, 1 H), 7.80 (d, *J* = 8.6 Hz, 1 H), 7.92 (s, 1 H), 8.07 (d, *J* = 8.4 Hz, 1 H) ppm.[75,76] ^{13}C NMR (126 MHz, DMSO-d_6/D_2O = 9:1, 25 °C): δ 31.2, 31.3, 33.0, 41.4, 44.3, 46.1, 47.7, 108.9, 115.5, 122.8, 123.3 (q, J_{CF} = 272.2 Hz), 124.4 (q, J_{CF} = 3.9 Hz), 127.7 (q, J_{CF} = 4.0 Hz), 127.7, 127.94 (q, J_{CF} = 33.14 Hz), 128.8, 131.7, 146.4, 153.1, 174.7 ppm.[76] ^{19}F {^{1}H} NMR (376 MHz, DMSO-d_6/D_2O = 9:1, 25 °C): δ -61.1 ppm.[76] HRMS (ESI): $[M+H]^+$ calcd. for $C_{20}H_{22}N_3O_3ClF_3$, 444.1296; found, 444.1296.

***rac*-(3*R*,5*R*)-(5-{2-[(*E*)-2-{[5-(2,4-Dichlorophenyl)furan-2-yl]methylidene}hydrazin-1-yl]ethyl}piperidine-3-carboxylic acid)–sodium chloride (1/3) (*rac*-18fy).[54]** According to **GP4** with *rac*-**13** x HCl, 5-(2,4-dichlorophenyl)-2-furaldehyde (**15fy**) and 1 M NaOD (30 µL) *rac*-**18fy** was obtained quantitatively in solution. Besides the major *E*-isomer the *Z*-isomer is present in 14%. ^{1}H NMR (500 MHz, DMSO-d_6/D_2O = 9:1, 25 °C): δ 1.09 (q, *J* = 12.5 Hz, 1 H), 1.43–1.58 (m, 2 H), 1.72–1.84 (m, 1 H), 2.11 (d, *J* = 13.3 Hz, 1 H), 2.30 (tt, *J* = 12.3/3.8 Hz, 1 H), 2.43 (t, *J* = 12.1 Hz, 1 H), 2.65 (t, *J* = 12.5 Hz, 1 H), 3.11–3.21 (m, 3

H), 3.28 (dd, *J* = 12.4/4.0 Hz, 1 H), 6.61 (d, *J* = 3.5 Hz, 1 H), 7.22 (d, *J* = 3.5 Hz, 1 H), 7.49 (s, 1 H), 7.52 (dd, *J* = 8.6/2.3 Hz, 1 H), 7.69 (d, *J* = 2.3 Hz, 1 H), 7.87 (d, *J* = 8.6 Hz, 1 H) ppm.[75,76] ^{13}C NMR (126 MHz, DMSO-d_6/D_2O = 9:1, 25 °C): δ 31.3, 31.3, 33.0, 41.4, 44.4, 46.1, 47.7, 108.9, 113.7, 123.3, 127.2, 127.9, 128.5, 129.3, 130.1, 132.0, 146.9, 152.2, 174.7 ppm.[76] HRMS (ESI): $[M+H]^+$ calcd. for $C_{19}H_{22}N_3O_3Cl_2$, 410.1033; found, 410.1032.

***rac*-(3*R*,5*S*)-[1-(*tert*-Butyl) 3-methyl 5-formylpiperidine-1,3-dicarboxylate] (*rac*-20)[44] and *rac*-(3*R*,5*R*)-[1-(*tert*-butyl) 3-methyl 5-formylpiperidine-1,3-dicarboxylate] (*rac*-21). 26** (1:1 *E*-/*Z*-mixture; 424 mg; 1.49 mmol) was dissolved in THF (15 mL). The solution was cooled to 0 °C and a 2 M aqueous HCl (2.5 mL; 5.0 mmol) was added. The mixture was stirred for 2 d, while the reaction was allowed to reach rt (0 °C → rt). It was quenched with $NaHCO_3$ (429 mg; 5.11 mmol) and concentrated under reduced pressure. H_2O (20 mL) was added to the residue and it was extracted with DCM (5 x 20 mL). The combined organic phases were dried over Na_2SO_4 and concentrated under reduced pressure. After purification by flash chromatography (*iso*-hexanes/EtOAc = 3:1) ***rac*-20** and ***rac*-21** were obtained in 1:1 mixture (according to ^{1}H NMR) as colorless oil (296 mg; 73%). ^{1}H NMR

(400 MHz, $C_2Cl_4D_2$, 80 °C): δ 1.43 (s, 9 H, *a* or *b*), 1.45 (s, 9 H, *a* or *b*), 1.59 (dt, *J* = 13.4/11.9 Hz, 1 H, *a*), 1.94 (ddd, *J* = 13.9/9.2/4.6 Hz, 1 H, *b*), 2.14–2.22 (m, 1 H, *b*), 2.32–2.54 (m, 3 H, *a* and *b*), 2.59–2.80 (m, 4 H, *a* and *b*), 3.31 (dd, *J* = 13.4/8.5 Hz, 1 H, *a*), 3.44 (dd, *J* = 13.8/4.3 Hz, 1 H, *b*), 3.68 (s, 3 H, *a* or *b*), 3.69 (s, 3 H, *a* or *b*), 3.79 (dd, *J* = 13.5/4.3 Hz, 1 H, *a*), 3.93 (dd, *J* = 13.7/5.2 Hz, 1 H, *b*), 4.22–4.33 (m, 2 H, *a* and *b*), 9.63 (d, *J* = 1 Hz, 1 H, *a*), 9.68 (s, 1 H, *b*) ppm. ^{13}C NMR (101 MHz, $C_2Cl_4D_2$, 80 °C): δ 25.8 (*b*), 27.5 (*a*), 28.4 (*a* or *b*), 28.5 (*a* or *b*), 38.3 (*b*), 40.7 (*a*), 43.3 (*b*), 43.6 (*a*), 45.7 (*a* or *b*), 45.8 (*a* or *b*), 45.8 (*a* or *b*), 47.6 (b), 51.9 (*a* or *b*), 52.0 (*a* or *b*), 80.4 (*a* or *b*), 80.5 (*a* or *b*), 154.3 (*a* or *b*), 154.4 (*a* or *b*), 172.8 (*a* or *b*), 173.1 (*a* or *b*), 200.7 (*a*), 201.1 (*b*) ppm. IR (film): $\tilde{\nu}$ 2977, 2955, 2933, 2871, 1735, 1694 cm^{-1}. HRMS (ESI): $[M+H]^+$ calcd. for $C_{13}H_{22}NO_5$, 272.1493; found, 272.1498.

***rac*-(3*R*,5*S*)-[1-(*tert*-Butyl) 3-methyl 5-hydroxypiperidine-1,3-dicarboxylate][41] (*rac*-23).** Methyl 5-hydroxynicotinate (**22**; 309 mg; 1.97 mmol), Rh on Al_2O_3 (94 mg; 0.046 mmol) and conc. H_2SO_4 (200 mg; 2.03 mmol) were suspended in MeOH (10 mL) under Ar. The mixture was hydrogenated (10 bar H_2) at 80 °C for 26 h. After cooling to rt the Rh on Al_2O_3 catalyst was filtered off and the solvent was concentrated in vacuum. The residue was

dissolved in dioxane (10 mL) and NEt_3 (1.1 mL; 7.8 mmol) and di-*tert*-butyl dicarbonate (401 mg; 1.80 mmol) were added. The reaction mixture was stirred at rt for 3 h before removing the solvent under vacuum. After purification by flash chromatography (*iso*-hexanes/EtOAc = 1:1) *rac*-**23** was obtained as white, amorphous solid (278 mg; 55%). ^{1}H NMR (400 MHz, $C_2Cl_4D_2$, 80 °C): δ 1.44 (s, 9 H), 1.55–1.70 (m, 1 H), 2.22 (d, *J* = 13.4 Hz, 1 H), 2.54 (tt, *J* = 9.3/4.1 Hz, 1 H), 2.75–2.86 (m, 1 H), 3.05 (d, *J* = 11.4 Hz, 1 H), 3.65 (tt, *J* = 8.9/3.9 Hz, 1 H), 3.69 (s, 3 H), 3.89 (d, *J* = 13.1 Hz, 1 H), 3.96 (d, *J* = 14.2 Hz, 1 H) ppm.[75] ^{13}C NMR (101 MHz, $C_2Cl_4D_2$, 80 °C): δ 28.4, 35.2, 40.0, 45.2, 50.6, 52.0, 65.5, 80.1, 154.5, 173.4 ppm. IR (KBr): $\tilde{\nu}$ 3463, 2986, 2957, 2936, 2870, 1732, 1673 cm^{-1}. HRMS (ESI): $[M+Na]^+$ calcd. for $C_{12}H_{21}NO_5Na$, 282.1312; found, 282.1312.

***rac*-(3*R*,5*R*)-[1-(*tert*-Butyl) 3-methyl 5-hydroxypiperidine-1,3-dicarboxylate] (*rac*-24).** *rac*-**24** was obtained as a side product from the preparation of *rac*-**23** as a colorless resin (97 mg; 19%). ^{1}H NMR (400 MHz, $C_2Cl_4D_2$, 80 °C): δ 1.44 (s, 9 H), 1.67 (br s, 1 H), 1.80 (t, *J* = 11.9 Hz, 1 H), 2.00 (d, *J* = 13.3 Hz, 1 H), 2.87 (tt, *J* = 9.8/4.1 Hz, 1 H), 3.02–3.17 (m, 2 H), 3.67 (s, 3 H), 3.75 (dd, *J* = 13.7/2.8 Hz, 1 H), 3.94–4.07 (m, 2 H) ppm.[75] ^{13}C NMR (101 MHz, $C_2Cl_4D_2$, 80 °C): δ 28.4, 34.0, 36.9, 45.8, 49.9, 51.7, 64.2, 80.1, 155.4,

173.6 ppm. IR (film): $\tilde{\nu}$ 3445, 2976, 2930, 1735, 1693, 1672 cm^{-1}. HRMS (ESI): $[M+Na]^+$ calcd. for $C_{12}H_{21}NO_5Na$, 282.1312; found, 282.1313.

***rac*-(3*R*)-(1-*tert*-Butyl 3-methyl 5-oxopiperidine-1,3-dicarboxylate)[42] (25).** *rac*-**23** (110 mg; 0.424 mmol) was dissolved in DCM (5 mL) and Dess-Martin periodinane (232 mg; 0.546 mmol) was added in portions over 45 min. After 2 h of stirring at rt another portion of Dess-Martin periodinane (131 mg; 0.309 mmol) was added and it was stirred for further 0.5 h. The mixture was concentrated in vacuum and after purification by flash chromatography (*iso*-hexanes/EtOAc = 3:7) **25** was obtained as a colorless resin (81 mg; 74%). ^{1}H NMR (400 MHz, $C_2Cl_4D_2$, 80 °C): δ 1.44 (s, 9 H), 2.58 (dd, J = 16.9/6.0 Hz, 1 H), 2.70 (dd, J = 16.9/7.3 Hz, 1 H), 3.03 (quin, J = 6.28 Hz, 1 H), 3.71 (s, 3 H), 3.76 (dd, J = 13.6/6.9 Hz, 1 H), 3.82 (dd, J = 13.7/5.0 Hz, 1 H), 3.94 (d, J = 18.9 Hz, 1 H), 3.99 (d, J = 18.9 Hz, 1 H) ppm. ^{13}C NMR (101 MHz, $C_2Cl_4D_2$, 80 °C): δ 28.3, 39.6, 40.1, 44.2, 52.3, 54.3, 80.9, 154.1, 172.4, 203.2 ppm. IR (film): $\tilde{\nu}$ 2978, 2956, 2934, 1737, 1698 cm^{-1}. HRMS (EI, 70 eV): M^+ calcd. for $C_{12}H_{19}NO_5$, 257.1263; found, 257.1268.

***rac*-(3*R*)-{1-(*tert*-Butyl) 3-methyl 5-[(*E*)-methoxymethylene]pipderidine-1,3-dicarboxylate} and *rac*-(3*R*)-1-{(*tert*-butyl) 3-methyl 5-[(*Z*)-**

methoxymethylene]pipderidine-1,3-dicarboxylate} (26).

(Methoxymethyl)triphenylphosphonium chloride (1.73 g; 4.95 mmol) and potassium *tert*-butoxide (524 mg; 4.58 mmol) were suspended in anhydrous THF (10 mL) under Ar. The mixture was stirred for 30 min at rt, cooled to -78 °C and then **25** (681 mg; 2.65 mmol), dissolved in anhydrous THF (5 mL), was added and stirred for further 75 min at -78 °C and 55 min at rt. Then the reaction was quenched with ammonium chloride (525 mg; 3.71 mmol), dissolved in H_2O (25 mL). The aqueous phase was extracted with DCM (5 x 20 mL). The combined organic phases were dried over Na_2SO_4 and concentrated under reduced pressure. After purification by flash chromatography (*iso*-hexanes/EtOAc = 5:1) **26** was obtained as colorless oil (432 mg; 57%) and as 1:1 mixture of the *E*- and *Z*-isomer according to ^{1}H NMR. ^{1}H NMR (400 MHz, $C_2Cl_4D_2$, 80 °C): δ 1.43 (s, 9 H, *E* or *Z*), 1.43 (s, 9 H, *E* or *Z*), 2.10 (t, *J* = 12.5 Hz, 1 H, *E*), 2.22 (t, *J* = 12.2 Hz, 1 H, *Z*), 2.37 (dd, *J* = 14.1/4.3 Hz, 1 H, *Z*), 2.43–2.52 (m, 2 H, *E* and *Z*), 2.93 (dd, *J* = 14.1/4.4 Hz, 1 H, *E*), 3.01–3.10 (m, 2 H, *E* and *Z*), 3.31 (d, *J* = 14.7 Hz, 1 H, *Z*), 3.36 (d, *J* = 14.1 Hz, 1 H, *E*), 3.55 (s, 3 H, *E*), 3.56 (s, 3 H, *E* or *Z*), 3.66 (s, 3 H, *E* or *Z*), 3.66 (s, 3 H, *E* or *Z*), 4.04–4.12 (m, 3 H, *E* and *Z*), 4.63 (d, *J* = 14.8 Hz, 1 H, *Z*), 5.81 (s, 1 H, *Z*), 5.97 (s, 1 H, *E*) ppm. ^{13}C

NMR (101 MHz, $C_2Cl_4D_2$, 80 °C): δ 26.3 (*E*), 28.5 (*E* or *Z*), 28.5 (*E* or *Z*), 30.5 (*Z*), 41.5 (*E*), 42.1 (*Z*), 42.3 (*Z*), 45.8 (*Z*), 46.2 (*E*), 46.7 (*E*), 51.6 (*E*), 51.6 (*Z*), 59.6 (*E*), 59.6 (*Z*), 79.6 (*E* or *Z*), 79.7 (*E* or *Z*), 109.6 (*E* or *Z*), 109.7 (*E* or *Z*), 141.9 (*Z*), 142.6 (*E*), 154.4 (*E* or *Z*), 154.7 (*E* or *Z*), 173.2 (*E* or *Z*), 173.2 (*E* or *Z*) ppm. IR (film): $\tilde{\nu}$ 2976, 2953, 2935, 2844, 1737, 1698 cm^{-1}. HRMS (EI, 70 eV): M^+ calcd. for $C_{14}H_{23}NO_5$, 285.1576; found, 285.1577.

***rac*-(3*R*,5*S*)-[1-(*tert*-Butyl) 3-methyl 5-(hydroxymethyl)piperidine-1,3-dicarboxylate][44] (*rac*-27) and *rac*-(3*R*,5*R*)-[1-(*tert*-butyl) 3-methyl 5-(hydroxymethyl)piperidine-1,3-dicarboxylate][48] (*rac*-28).** *rac*-**20** and *rac*-**21** (in 1:1 mixture; 191 mg; 0.703 mmol) were dissolved in ethanol (5 mL) and cooled to 0 °C. Sodium borohydride (80 mg; 2.1 mmol) was added to the solution and it was stirred for 1 h. The reaction was quenched with ammonium chloride (202 mg; 3.78 mmol), dissolved in H_2O (25 mL), and it was extracted with DCM (5 x 20 mL). The combined organic phases were dried over Na_2SO_4 and concentrated under reduced pressure. After purification by flash chromatography (*iso*-hexanes/EtOAc = 2:1) *rac*-**27** and *rac*-**28** were obtained in 1:1 mixture (according to ^1H NMR) as colorless oil (145 mg; 76%). ^1H NMR (400 MHz, $C_2Cl_4D_2$, 80 °C): δ 1.25–1.36

(m, 1 H, *a*), 1.44 (s, 9 H, *a* or *b*), 1.44 (s, 9 H, *a* or *b*), 1.62–1.76 (m, 2 H, *a* and *b*), 1.86–1.99 (m, 2 H, *b*), 2.11 (dtt, *J* = 13.1/3.6/1.7 Hz, 1 H, *a*), 2.35–2.51 (m, 2 H, *a*), 2.58 (tt, *J* = 8.4/4.4 Hz, 1 H, *b*), 2.72 (dd, *J* = 13.2/11.3 Hz, 1 H, *a*), 3.31 (dd, *J* = 13.5/3.7 Hz, 1 H, *b*), 3.38–3.51 (m, 6 H, *a* and *b*), 3.66 (s, 3 H, *a* or *b*), 3.67 (s, 3 H, *a* or *b*), 3.72 (dd, *J* = 13.5/4.4 Hz, 1 H, *b*), 4.09–4.16 (m, 1 H, *a*), 4.22–4.30 (m, 1 H, *a*) ppm.[75] ^{13}C NMR (101 MHz, $C_2Cl_4D_2$, 80 °C): δ 28.4 (*a* or *b*), 28.5 (*a* or *b*), 28.5 (*b*), 30.4 (*a*), 35.2 (*b*), 38.0 (*a* or *b*), 38.1 (*a* or *b*), 41.3 (*a*), 45.3 (*b*), 45.9 (*a* or *b*), 46.0 (*a* or *b*), 46.7 (*a*), 51.7 (*a*), 51.7 (*b*), 63.2 (*a*), 65.1 (*b*), 79.8 (*a* or *b*), 79.9 (*a* or *b*), 154.6 (*a* or *b*), 155.0 (*a* or *b*), 173.4 (*a* or *b*), 173.5 (*a* or *b*) ppm. IR (film): $\tilde{\nu}$ 3450, 2976, 2932, 2868, 1736, 1691, 1672 cm^{-1}. HRMS (EI, 70 eV): M^+ calcd. for $C_{13}H_{23}NO_5$, 273.1576; found, 273.1576.

***rac*-(3*R*,5*S*)-[1-(*tert*-Butyl) 3-methyl 5-{[1-(*tert*-butoxycarbonyl)hydrazinyl]methyl}piperidine-1,3-dicarboxylate] (*rac*-30).** *rac*-**27** and *rac*-**28** (in 1:1 mixture; 464 mg; 1.70 mmol), *N*-(*tert*-butoxycarbonyl)aminophthalimide[47] (**29**; 710 mg; 2.71 mmol) and triphenylphosphine (1.06 g; 3.94 mmol) were dissolved in anhydrous THF (20 mL) under Ar. The solution was cooled to 0 °C and diisopropyl azodicarboxylate (1.0 mL; 4.8 mmol) was added dropwise over 30 min under stirring.

After additional 75 min of stirring the reaction mixture was concentrated under reduced pressure. The crude intermediate was purified by flash chromatography (*iso*-hexanes/EtOAc = 3:1) and the resulting residue was dissolved in THF (20 mL) and cooled to 0 °C. Methylhydrazine (0.50 mL; 9.6 mmol) was added and after 110 min of stirring another portion of methylhydrazine (0.10 mL; 1.9 mmol) was added. The reaction mixture was stirred for further 10 min at 0 °C and then concentrated under reduced pressure. After purification by flash chromatography (*iso*-hexanes/EtOAc = 1:1) *rac*-**30** was obtained as colorless oil (249 mg; 38%). ^{1}H NMR (400 MHz, $C_2Cl_4D_2$, 80 °C): δ 1.15–1.31 (m, 1 H), 1.44 (s, 9 H), 1.46 (s, 9 H), 1.82–1.95 (m, 1 H), 2.02–2.09 (m, 1 H), 2.31 (dd, *J* = 13.2/11.5 Hz, 1 H), 2.45 (tt, *J* = 11.8/4.0 Hz, 1 H), 2.65 (dd, *J* = 13.2/11.5 Hz, 1 H), 3.20 (dd, *J* = 14.0/6.1 Hz, 1 H), 3.27 (dd, *J* = 14.0/7.4 Hz, 1 H), 3.67 (s, 3 H), 3.91 (br s, 2 H), 4.06 (dt, *J* = 13.2/1.8 Hz, 1 H), 4.31 (dt, *J* = 13.2 Hz, 1 H) ppm.[75] ^{13}C NMR (101 MHz, $C_2Cl_4D_2$, 80 °C): δ 28.4, 28.5, 31.9, 34.9, 41.6, 45.9, 47.8, 51.6, 53.7, 79.8, 80.7, 154.4, 156.7, 173.3 ppm. IR (film): $\tilde{\nu}$ 3334, 2975, 2931, 1736, 1693, 1631 cm^{-1}. HRMS (EI, 70 eV): M^+ calcd. for $C_{18}H_{33}N_3O_6$, 387.2369; found, 387.2369.

rac-(3_R_,5_R_)-[1-(_tert_-Butyl) 3-methyl 5-{[1-(_tert_-butoxycarbonyl)hydrazinyl]methyl}piperidine-1,3-dicarboxylate] (_rac_-31). _rac_-**31** was obtained as additional product in the synthesis of _rac_-**30** as colorless oil (282 mg; 43%). ^{1}H NMR (400 MHz, $C_2Cl_4D_2$, 80 °C): δ 1.43 (s, 9 H), 1.45 (s, 9 H), 1.53–1.64 (m, 1 H), 1.85 (ddd, J = 12.7/8.0/4.3 Hz, 1 H), 2.15–2.25 (m, 1 H), 2.69 (ddt, J = 11.3/8.1/4.6 Hz, 1 H), 3.13–3.22 (m, 2 H), 3.36–3.45 (m, 2 H), 3.50–3.69 (m, 5 H), 3.98 (br s, 2 H) ppm.[75] ^{13}C NMR (101 MHz, $C_2Cl_4D_2$, 80 °C): δ 28.4, 28.4, 29.0, 31.7, 38.1, 45.6, 46.8, 51.5, 52.1, 79.6, 80.6, 154.5, 156.7, 173.6 ppm. IR (film): $\tilde{\nu}$ 3334, 3224, 2976, 2932, 2868, 1736, 1694 cm^{-1}. HRMS (EI, 70 eV): M^+ calcd. for $C_{18}H_{33}N_3O_6$, 387.2369; found, 387.2379.

rac-(3_R_,5_S_)-{1-[(_tert_-Butoxy)carbonyl] 5-({1-[(_tert_-butoxy)carbonyl]hydrazinyl}methyl)piperidine-3-carboxylic acid} (_rac_-32). _rac_-**30** (316 mg; 0.816 mmol) was dissolved in MeOH (10 mL), cooled to 0 °C and a 1 M aqueous NaOH (3.0 mL; 3.0 mmol) was added. The mixture was stirred for 15 h, while the reaction was allowed to reach rt (0 °C → rt). Then it was concentrated under reduced pressure, diluted with H_2O (30 mL), washed with DCM (3 x 20 mL) and acidified with phosphoric acid (85%; 0.25 mL; 3.7 mmol). The aqueous phase was extracted with DCM (5 x 20 mL). The

combined organic phases were dried over Na_2SO_4 and concentrated under reduced pressure. *rac*-**32** was obtained as colourless resin (313 mg; quant.). ^{1}H NMR (400 MHz, $C_2Cl_4D_2$, 80 °C): δ 1.34–1.42 (m, 1 H), 1.54 (s, 9 H), 1.56 (s, 9 H), 1.92–2.07 (m, 1 H), 2.20 (dm, *J* = 13.3 Hz, 1 H), 2.42 (dd, *J* = 13.2/11.5 Hz, 1 H), 2.59 (tt, *J* = 11.7/3.9 Hz, 1 H), 2.78 (dd, *J* = 13.2/11.5 Hz, 1 H), 3.31 (dd, *J* = 14.0/6.2 Hz, 1 H), 3.38 (dd, *J* = 14.0/7.2 Hz, 1 H), 4.18 (dm, *J* = 13.2 Hz, 1 H), 4.44 (dm, *J* = 13.1 Hz, 1 H) ppm.[75] ^{13}C NMR (101 MHz, $C_2Cl_4D_2$, 80 °C): δ 28.4, 28.5, 31.8, 34.9, 41.0, 45.7, 47.7, 53.7, 80.0, 80.9, 154.5, 156.8, 175.2 ppm. IR (film): $\tilde{\nu}$ 3434, 2979, 2934, 1729, 1697 cm^{-1}. HRMS (ESI): $[M+H]^+$ calcd. for $C_{17}H_{32}N_3O_6$, 374.2286; found, 374.2290.

rac-(3*R*,5*R*)-{1-(*tert*-Butyl) 3-methyl 5-[(*E*)-2-methoxyethenyl]piperidine-1,3-dicarboxylate} and rac-(3*R*,5*R*)-{1-(*tert*-butyl) 3-methyl 5-[(*Z*)-2-methoxyethenyl]piperidine-1,3-dicarboxylate} (*rac*-33).

(Methoxymethyl)triphenylphosphonium chloride (2.85 g; 8.16 mmol) and potassium *tert*-butoxide (856 mg; 7.48 mmol) were suspended in anhydrous THF (23 mL) under Ar. The mixture was stirred at rt for 30 min, cooled to 0 °C and then *rac*-**20** and *rac*-**21** (in 1:1 mixture; 1.15 g; 4.25 mmol), dissolved in anhydrous THF (10 mL), were added. It was

stirred for further 80 min at 0 °C and 20 min at rt. Then the reaction was quenched with ammonium chloride (905 mg; 16.9 mmol), dissolved in H_2O (30 mL). *iso*-hexane (15 mL) was added, the phases were separated and the aqueous phase was further extracted with DCM (4 x 25 mL). The combined organic phases were dried over Na_2SO_4 and concentrated under reduced pressure. After purification by flash chromatography on silica gel (EtOAc/*iso*-hexane = 1:5) *rac*-**33** was obtained as colorless oil (614 mg; 48 %) and as 1:0.43 mixture of the *E*- and *Z*-isomer according to ^{1}H NMR. ^{1}H NMR (400 MHz, $C_2Cl_4D_2$, 80 °C): δ 1.25–1.39 (m, 1 H + 0.43 x 1 H, *E* and *Z*), 1.54 (s, 0.43 x 9 H, *Z*), 1.54 (s, 9 H, *E*), 2.00–2.15 (m, 2 H + 0.43 x 1 H, *E* and *Z*), 2.28–2.38 (m, 1 H + 0.43 x 1 H, *E* and *Z*), 2.40–2.58 (m, 1 H + 0.43 x 2 H, *E* and *Z*), 2.60–2.70 (m, 1 H + 0.43 x 1 H, *E* and *Z*), 3.48 (s, 3 H, *E*), 3.56 (s, 0.43 x 3 H, *Z*), 3.65 (s, 0.43 x 3 H, *Z*), 3.66 (s, 3 H, *E*), 3.96–4.05 (m, 1 H + 0.43 x 1 H, *E* and *Z*), 4.07 (dd, *J* = 8.2/6.3 Hz, 0.43 x 1 H, *Z*), 4.21–4.32 (m, 1 H + 0.43 x 1 H, *E* and *Z*), 4.57 (dd, *J* = 12.7/7.5 Hz, 1 H, *E*), 5.88 (dd, *J* = 6.3/1.1 Hz, 0.43 x 1 H, *Z*), 6.32 (dd, *J* = 12.7/0.8 Hz, 1 H, *E*) ppm. ^{13}C NMR (101 MHz, $C_2Cl_4D_2$, 60 °C): δ 28.4 (*E*), 28.4 (*Z*), 31.7 (*Z*), 34.2 (*Z*), 34.7 (*E*), 35.0 (*E*), 41.4 (*Z*), 41.5 (*E*), 45.4 (*E*), 45.4 (*Z*), 50.0 (*E*), 50.0 (*Z*), 51.6 (*Z*), 51.7 (*E*), 56.1 (*E*), 59.7 (*Z*), 79.6 (*Z*), 79.7 (*E*), 104.2 (*E*), 106.8

(*Z*), 147.4 (*Z*), 148.1 (*E*), 154.4 (*E*), 154.5 (*Z*), 173.4 (*E*), 173.5 (*Z*) ppm. IR (film): $\tilde{\nu}$ 2976, 2952, 2935, 2861, 1737, 1694, 1655 cm^{-1}. HRMS (ESI): $[M+H]^+$ calcd. for $C_{15}H_{26}NO_5$, 300.1806; found, 300.1806.

***rac*-(3*R*,5*S*)-{1-(*tert*-Butyl) 3-methyl 5-[(*E*)-2-methoxyethenyl]piperidine-1,3-dicarboxylate} and *rac*-(3*R*,5*S*)-{1-(*tert*-butyl) 3-methyl 5-[(*Z*)-2-methoxyethenyl]piperidine-1,3-dicarboxylate} (*rac*-34).** *rac*-**34** was obtained as additional product in the synthesis of *rac*-**33** as colorless oil (417 mg; 33%) and as 1:0.27 mixture of the *E*- and *Z*-isomer according to ^{1}H NMR. ^{1}H NMR (400 MHz, $C_2Cl_4D_2$, 80 °C): δ 1.43 (s, 0.27 x 9 H, *Z*), 1.43 (s, 9 H, *E*), 1.59 (ddd, *J* = 13.1/8.0/4.5 Hz, 1 H, *E*), 1.74 (ddd, *J* = 12.9/6.7/4.4 Hz, 0.27 x 1 H, *Z*), 1.89 (ddd, *J* = 12.8/8.3/4.3 Hz, 0.27 x 1 H, *Z*), 1.99 (ddd, *J* = 13.2/7.0/4.2 Hz, 1 H, *E*), 2.42 (qt, *J* = 7.7/4.0 Hz, 1 H, *E*), 2.54–2.70 (m, 1 H + 0.27 x 2 H, *E* and *Z*), 2.79–2.90 (m, 0.27 x 1 H, *Z*), 3.06 (dd, *J* = 13.0/7.4 Hz, 1 H, *E*), 3.26–3.32 (m, 0.27 x 1 H, *Z*), 3.40–3.54 (m, 5 H + 0.27 x 2 H, *E* and *Z*), 3.57 (s, 0.27 x 3 H, *Z*), 3.59–3.76 (m, 4 H + 0.27 x 4 H, *E* and *Z*), 4.24 (dd, *J* = 8.0/6.3 Hz, 0.27 x 1 H, *Z*), 4.65 (dd, *J* = 12.7/7.6 Hz, 1 H, *E*), 5.87 (dd, *J* = 6.3/1.3 Hz, 0.27 x 1 H, *Z*), 6.34 (dd, *J* = 12.8/1.0 Hz, 1 H, *E*) ppm. ^{13}C NMR (101 MHz, $C_2Cl_4D_2$, 60 °C): δ 28.4 (*E*), 28.4 (*Z*), 28.9 (*Z*), 31.7

(*E*), 32.5 (*Z*), 33.4 (*E*), 38.3 (*E*), 38.3 (*Z*), 45.2 (*E*), 45.2 (*Z*), 49.3 (*E*), 49.3 (*Z*), 51.6 (*E*), 51.6 (*Z*), 56.1 (*E*), 59.7 (*Z*), 79.3 (*Z*), 79.4 (*E*), 104.0 (*E*), 106.5 (*Z*), 147.0 (*Z*), 148.1 (*E*), 154.4 (*E*), 154.7 (*Z*), 173.6 (*E*), 173.9 (*Z*) ppm. IR (film): $\tilde{\nu}$ 2975, 2951, 2933, 2860, 1736, 1694, 1654 cm^{-1}. HRMS (ESI): $[M+H]^+$ calcd. for $C_{15}H_{26}NO_5$, 300.1806; found, 300.1808.

rac-(3*R*,5*R*)-[1-(*tert*-Butyl) 3-methyl 5-(2-oxoethyl)piperidine-1,3-dicarboxylate] (_rac_-35). According to **GP2** with _rac_-**33** (568 mg; 1.90 mmol) and 2 M aqueous HCl (3.5 mL; 7.0 mmol) and a reaction time of 7 h. _rac_-**35** was obtained as a colorless oil (435 mg; 80%). ^{1}H NMR (400 MHz, $C_2Cl_4D_2$, 80 °C): δ 1.28 (q, *J* = 12.4 Hz, 1 H), 1.45 (s, 9 H), 1.97–2.09 (m, 1 H), 2.15 (dtt, *J* = 13.1/3.7/1.8 Hz, 1 H), 2.22–2.38 (m, 3 H), 2.50 (tt, *J* = 11.7/4.0 Hz, 1 H), 2.69 (dd, *J* = 13.2/11.5 Hz, 1 H), 3.67 (s, 3 H), 4.07 (dm, *J* = 13.0 Hz, 1 H), 4.29 (dm, *J* = 13.4 Hz, 1 H), 9.74 (t, *J* = 1.8 Hz, 1 H) ppm. ^{13}C NMR (101 MHz, $C_2Cl_4D_2$, 80 °C): δ 28.5, 30.4, 33.8, 41.5, 45.7, 47.4, 49.0, 51.7, 80.1, 154.4, 173.0, 200.0 ppm. IR (film): $\tilde{\nu}$ 2977, 2953, 2933, 2863, 2724, 1733, 1693 cm^{-1}. HRMS (ESI): $[M+H]^+$ calcd. for $C_{14}H_{24}NO_5$, 286.1649; found, 286.1656.

rac-(3*R*,5*S*)-[1-(*tert*-Butyl) 3-methyl 5-(2-oxoethyl)piperidine-1,3-dicarboxylate] (_rac_-36). According to **GP2** with _rac_-**34** (326 mg; 1.09 mmol) and 2 M aqueous HCl (2.0 mL;

4.0 mmol) and a reaction time of 8.5 h. *rac*-**36** was obtained as a colorless oil (272 mg; 88%). ^{1}H NMR (400 MHz, $C_2Cl_4D_2$, 120 °C): δ 1.43 (s, 9 H), 1.61 (ddd, *J* = 13.6/6.1/4.4 Hz, 1 H), 1.99 (ddd, *J* = 13.6/8.2/3.8 Hz, 1 H), 2.24–2.44 (m, 3 H), 2.58 (tt, *J* = 8.1/4.4 Hz, 1 H), 3.19 (dd, *J* = 13.4/5.9 Hz, 1 H), 3.43 (dd, *J* = 13.3/3.3 Hz, 1 H), 3.54 (dd, *J* = 13.5/7.1 Hz, 1 H), 3.60–3.67 (m, 4 H), 9.74 (t, *J* = 1.7 Hz, 1 H) ppm. ^{13}C NMR (101 MHz, $C_2Cl_4D_2$, 80 °C): δ 27.5, 28.4, 31.9, 38.2, 45.5, 45.9, 48.1, 51.7, 79.8, 154.5, 173.2, 200.4 ppm. IR (film): $\tilde{\nu}$ 2976, 2952, 2932, 2868, 2723, 1731, 1693 cm^{-1}. HRMS (ESI): $[M+H]^+$ calcd. for $C_{14}H_{24}NO_5$, 286.1649; found, 286.1655.

***rac*-(3*R*,5*R*)-{1-(*tert*-Butyl) 3-methyl 5-[2-({[(*tert*-butoxy)carbonyl]amino}amino)ethyl]piperidine-1,3-dicarboxylate} (*rac*-37).** According to **GP3** with *rac*-**35** (86 mg ; 0.30 mmol), *tert*-butyl carbazate (66 mg; 0.49 mmol), AcOH (0.043 mL ; 0.75 mmol) and $NaBH_3CN$ (81 mg ; 1.2 mmol; added in three portions). *rac*-**37** was obtained as a colorless oil (90 mg; 74%). ^{1}H NMR (400 MHz, $C_2Cl_4D_2$, 80 °C): δ 1.18 (q, *J* = 12.3 Hz, 1 H), 1.26–1.38 (m, 2 H), 1.44 (s, 9 H), 1.44 (s, 9 H), 1.50–1.58 (m, 1 H), 2.12 (dtt, *J* = 12.6/3.4/1.8 Hz, 1 H), 2.24 (dd, *J* = 12.9/11.8 Hz, 1 H), 2.43 (tt, *J* = 11.8/4.0 Hz, 1 H), 2.66 (dd, *J* = 12.9/11.8 Hz, 1 H), 2.85 (dd, *J* = 12.7/6.9 Hz, 1 H), 2.89

(dd, *J* = 12.8/7.5 Hz, 1 H), 3.66 (s, 3 H), 4.06 (dm, *J* = 13.1 Hz, 1 H), 4.27 (dm, *J* = 13.1 Hz, 1 H) ppm.[75] ^{13}C NMR (101 MHz, $C_2Cl_4D_2$, 80 °C): δ 28.4, 28.5, 31.9, 33.5, 34.2, 41.7, 45.8, 49.3, 49.6, 51.6, 79.7, 80.4, 154.5, 156.6, 173.4 ppm. IR (film): $\tilde{\nu}$ 3329, 2976, 2930, 2868, 1736, 1696 cm^{-1}. HRMS (ESI): $[M+H]^+$ calcd. for $C_{19}H_{36}N_3O_6$, 402.2599; found, 402.2599.

***rac*-(3*R*,5*S*)-{1-(*tert*-Butyl) 3-methyl 5-[2-({[(*tert*-butoxy)carbonyl]amino}amino)ethyl]piperidine-1,3-dicarboxylate} (*rac*-38).** According to **GP3** with *rac*-**36** (115 mg; 0.403 mmol), *tert*-butyl carbazate (89 mg; 0.66 mmol), AcOH (0.057 mL; 1.0 mmol) and $NaBH_3CN$ (112 mg; 1.69 mmol; added in three portions). *rac*-**38** was obtained as a colorless oil (125 mg; 77%). ^{1}H NMR (400 MHz, $C_2Cl_4D_2$, 120 °C): δ 1.29–1.40 (m, 2 H), 1.43 (s, 9 H), 1.44 (s, 9 H), 1.51–1.61 (m, 1 H), 1.80–1.90 (m, 1 H), 1.95 (ddd, *J* = 12.6/7.7/4.2 Hz, 1 H), 2.52–2.63 (m, 1 H), 2.81–2.94 (m, 2 H), 3.14 (dd, *J* = 13.2/6.6 Hz, 1 H), 3.40 (dd, *J* = 13.2/3.7 Hz, 1 H), 3.55 (dd, *J* = 13.4/6.6 Hz, 1 H), 3.58 (dd, *J* = 13.5/5.1 Hz, 1 H), 3.65 (s, 3 H), 5.94 (br s, 1 H) ppm.[75] ^{13}C NMR (101 MHz, $C_2Cl_4D_2$, 80 °C): δ 28.4, 28.5, 30.1, 30.8, 32.4, 38.2, 45.6, 48.4, 49.9, 51.6, 79.5, 80.3,

154.6, 156.6, 173.6 ppm. IR (film): $\tilde{\nu}$ 3320, 2976, 2930, 2861, 1735, 1796 cm^{-1}. HRMS (ESI): $[M+H]^+$ calcd. for $C_{19}H_{36}N_3O_6$, 402.2599; found, 402.2603.

Aldehydes. Synthetic protocols and detailed analytical data for aldehydes are provided in the Supporting Information.

MS binding experiments. mGAT1 membrane preparation. Membrane preparations of HEK293 cells stably expressing mGAT1[55] were prepared and applied as previously described.[35,51,77]

Library screening. Library screening experiments were basically performed as reported[35,51] except for varying hydrazine and aldehyde concentrations and buffer composition: Quadruplicate samples in a total volume of 250 µL in 1.2 mL polysterene 96-deep-well plates (Sarstedt) were employed. The incubation buffer contained 12.5 mM Na_2HPO_4 x 2 H_2O, 12.5 mM NaH_2PO_4 x H_2O, 1 M NaCl and 200 µM sodium L-ascorbate and the pH was adjusted to 7.1 with 2 M NaOH. Solutions were added as 10-fold concentrated stock solutions and all samples contained 1% DMSO (final concentration). Aldehydes were applied in a final concentration of 1.0 µM per sample (with each aldehyde library representing a mixture of eight different aldehydes) and hydrazines (*rac*-**11**, *rac*-

12, *rac*-**13** or *rac*-**14**, applied as hydrochlorides)[49] were applied in 200 µM. Directly after combining the hydrazine and aldehydes the mGAT1 membrane preparation was added, which started the first incubation period of 4 h at 37 °C in a shaking water bath (for library generation). Then MS marker **6** was added in a concentration of 20 nM (final concentration in the sample) starting the second incubation period of 40 min at 37 °C. Total binding was determined with analogously constituted samples lacking any inhibitor and nonspecific binding was determined in the presence of 100 mM GABA. All experiments additionally obtained matrix blanks, zero samples and matrix standards. The incubation was terminated by vacuum filtration (96-well filter plate, Acroprep, glass fiber, 1.0 µm, 350 µL; Pall). After five washing steps with ice-cold aqueous 1 M NaCl, the filter plates were dried at 50 °C for 60 min and cooled to room temperature. The marker **6** was subsequently liberated by elution with MeOH and the eluate was collected in a 96-deep-well plate. To each sample (except the matrix blanks) 200 µL of 1 nM [$^2H_{10}$]NO711 in MeOH was added as internal standard. For calibration, blank matrix was supplemented with 200 µL of methanolic calibration standards with 20 pM, 50 pM, 100 pM, 200 pM, 500 pM, 1.0 nM, 2.5 nM and 5.0 nM NO711, respectively (these samples were employed for

generating calibration curves for marker quantitation). All samples were dried to completeness at 50 °C for 16 h and subsequently reconstituted in 200 µL of 10 mM ammonium formate buffer (pH 7.0) containing 5% MeOH. Quantification was performed by LC-ESI-MS/MS. As control, analogous samples were employed in the library screening experiments for characterizing specific binding of pure aldehyde libraries and pure hydrazines (*rac*-**11**, *rac*-**12**, *rac*-**13** or *rac*-**14**, applied as hydrochlorides),[49] respectively.

Deconvolution experiments. The deconvolution experiments were analogously performed as the library screening experiments (as described above) but instead of a mixture of eight aldehydes single aldehydes (1.0 µM per sample) were applied.

Competition experiments for establishing binding affinities of hydrazones. Full-scale MS binding experiments were performed as previously described,[38,77] applying pure hydrazones[54] and the incubation buffer as described under “Library screening”.

Saturation experiments for investigation of test compounds’ mode of interaction. MS based saturation experiments with NO711 as reporter ligand (concentration range: 2.5 nM–480 nM) addressing mGAT1 were performed as previously described.[38,77] Pure hydrazones[54] and tiagabine were added in the desired concentrations to the binding

samples before incubation was started by addition of the mGAT1 membrane preparation. All other conditions (e.g. incubation buffer, filtration and washing of binding samples, drying of eluates and reconstitution of samples) were exactly the same as described under “Library screening”.

LC-ESI-MS/MS. Quantification by LC-ESI-MS/MS was performed on an API 3200 or 3200 Q TRAP triple-quadrupole mass spectrometer (AB Sciex). The injection volume was always 30 µL and the LC conditions were exactly as described previously.[38] Detailed instrument settings of the mass spectrometers are specified in the Supporting Information.

Data Analysis in mGAT1 MS Binding Assays. Data analysis was performed as previously described.[35,38,51,77] Binding affinities for test compounds are expressed as pK_i values (with K_i values calculated according to Cheng and Prussoff;[78] taking into account that the investigated test compounds and NO711 may not address the same binding site, the K_i values could be considered as apparent K_i values). Affinities (K_d) for NO711 and densities of binding sites (B_{max}) in the absence or presence of test compounds were calculated from saturation isotherms. B_{max} values are given in [pmol/(mg protein)], K_d

values in [nM]. All results represent means±SEM, determined in at least three separate experiments. To distinguish between competitive and non-competitive binding interactions between test compounds and the reporter ligand NO711 a Schild-like coefficient was calculated according to Hulme and Trevethick[58] with coefficient = [log ($K_{d\_NO711\_app}/K_{d\_NO711}$ -1)$_{higher\ concentrated\ test\ compound}$ - log ($K_{d\_NO711\_app}/K_{d\_NO711}$ -1)$_{lower\ concentrated\ test\ compound}$] / [log (higher concentration test compound) - log (lower concentration test compound)]

GABA uptake assays. [^{3}H]GABA uptake assays were performed as previously described[55] except that 200 µM sodium L-ascorbate was added to all samples as antioxidant.

MS Transport Assays. Competitive MS Transport Assays. Competitive MS Transport Assays were performed as reported[64,65] except that sodium L-ascorbate (200 µM) was added to all samples (including controls) as antioxidant.

Saturation experiments for investigation of test compound's mode of interaction by means of MS Transport Assays. Saturation experiments by means of MS Transport Assays with COS cells stably expressing hGAT1 were performed as previously

described[64,65] except that sodium L-ascorbate (200 µM) was added to all samples as antioxidant. Pure hydrazones *rac*-**16gf** and *rac*-**16gg** and tiagabine (**5**), respectively, were added in the desired concentrations to the samples containing the COS-hGAT1 cells and after preincubation for 25 min the addition of ($^2H_6$)GABA started the uptake. V_{max} and K_m values in the absence or presence of test compound were calculated from saturation isotherms. V_{max} values are given in [amol/cell • min], K_m values in [µM]. All results represent means±SEM, determined in three separate experiments.

ASSOCIATED CONTENT

Supporting Information

The Supporting Information is available free of charge on the ACS Publications website at: http://pubs.acs.org

General procedure for the synthesis of new aldehydes (**15fd**, **15ff**, **15fh**, **15fi**, **15fn**, **15fp**, **15fs** and **15gr**) with detailed analytical data of aldehydes, information regarding the reaction progress of hydrazone formation, control experiments for library screening with individual building blocks, control experiments for hydrazone stability in incubation

buffers, control experiments for investigation of test compound's mode of interaction, detailed instrument settings of the mass spectrometers and NMR spectra of compounds (PDF)

Molecular-formula strings (CSV)

Coordinates of the hGAT1 model (PDB)

AUTHOR INFORMATION

Corresponding Author

*Phone: +49 2180 77249. Fax +49 2180 77247. E-mail: Klaus.Wanner@cup.uni-muenchen.de

Notes

The authors declare no competing financial interest.

ACKNOWLEDGEMENTS

We like to thank Simone Huber, Dr. Karuna Bhokare, Hans Brabec and Janine Piecek for the help of compiling aldehyde libraries, Dr. Lars Allmendinger and Dr. Jörg Pabel for

technical assistance, and Silke Duensing-Kropp, Tanja Franz and Miriam Sandner for performing GABA uptake assays and MS Transport Assays.

ABBREVIATIONS USED

BGT, betaine/γ-aminobutyric acid transporter; DCC, dynamic combinatorial chemistry; DIAD, diisopropyl azodicarboxylate; dm, doublet of a multiplet (NMR); GAT, γ-aminobutyric acid transporter; GP, general procedure; HUGO, human genome organization; LeuT, leucine transporter; PAINS, pan assay interference compounds; SLC6, solute carrier 6 gene family.

REFERENCES

(1) Bradford, H. F. Glutamate, GABA and epilepsy. *Prog. Neurobiol.* **1995**, *47*, 477–511.

(2) Treiman, D. M. GABAergic mechanisms in epilepsy. *Epilepsia* **2001**, *42*, 8–12.

(3) Kleppner, S. R.; Tobin, A. J. GABA signalling: therapeutic targets for epilepsy, Parkinson's disease and Huntington's disease. *Expert Opin. Ther. Targets* **2001**, *5*, 219–239.

(4) Ishiwari, K.; Mingote, S.; Correa, M.; Trevitt, J. T.; Carlson, B. B.; Salamone, J. D. The GABA uptake inhibitor β-alanine reduces pilocarpine-induced tremor and increases extracellular GABA in substantia nigra pars reticulata as measured by microdialysis. *J. Neurosci. Methods* **2004**, *140*, 39–46.

(5) Kalueff, A. V.; Nutt, D. J. Role of GABA in anxiety and depression. *Depress. Anxiety* **2007**, *24*, 495–517.

(6) Todorov, A. A.; Kolchev, C. B.; Todorov, A. B. Tiagabine and gabapentin for the management of chronic pain. *Clin. J. Pain* **2005**, *21*, 358–361.

(7) Daemen, M. A.; Hoogland, G.; Cijntje, J. M.; Spincemaille, G. H. Upregulation of the GABA-transporter GAT-1 in the spinal cord contributes to pain behaviour in experimental neuropathy. *Neurosci. Lett.* **2008**, *444*, 112–115.

(8) Kowalczyk, P.; Kulig, K. GABA system as target for new drugs. *Curr. Med. Chem*. **2014**, *21*, 3294–3309.

(9) Kristensen, A. S.; Andersen, J.; Jørgensen, T. N.; Sørensen, L.; Eriksen, J.; Loland, C. J.; Strømgaard, K.; Gether, U. SLC6 neurotransmitter transporters: structure, function, and regulation. *Pharmacol. Rev.* **2011**, *63*, 585–640.

(10) Madsen, K. K.; Clausen, R. P.; Larsson, O. M.; Krogsgaard-Larsen, P.; Schousboe, A.; White, H. S. Synaptic and extrasynaptic GABA transporters as targets for anti-epileptic drugs. *J. Neurochem*. **2009**, *109*, 139−144.

(11) Wellendorph, P.; Jacobsen, J.; Skovgaard-Petersen, J.; Jurik, A.; Vogensen, S. B.; Ecker, G.; Schousboe, A.; Krogsgaard-Larsen, P.; Clausen, R. P. γ-Aminobutyric Acid and Glycine Neurotransmitter Transporters. In *Transporters as Drug Targets*, 1st ed.; Ecker, G. F., Clausen, R. P., Sitte, H. H., Eds.; Wiley-VCH: Weinheim, 2017; pp 69−106.

(12) Krogsgaard-Larsen, P.; Frølund, B.; Frydenvang, K. GABA uptake inhibitors. Design, molecular pharmacology and therapeutic aspects. *Curr. Pharm. Des*. **2000**, *6*, 1193−1209.

(13) Zhou, Y.; Danbolt, N. C. GABA and glutamate transporters in brain. *Front. Endocrinol*. **2013**, 4, 165.

(14) Krogsgaard-Larsen, P.; Johnston, G. A. R. Inhibition of GABA uptake in rat brain slices by nipecotic acid, various isoxazoles and related compounds. *J. Neurochem*. **1975**, *25*, 797−802.

(15) Krogsgaard-Larsen, P.; Falch, E.; Larsson, O. M.; Schousboe, A. GABA uptake inhibitors: relevance to antiepileptic drug research. *Epilepsy Res*. **1987**, *1*, 77–93.

(16) Yunger, L. M.; Fowler, P. J.; Zarevics, P.; Setler, P. E. Novel inhibitors of gamma-aminobutyric acid (GABA) uptake: anticonvulsant actions in rats and mice. *J. Pharmacol. Exp. Ther.* **1984**, *228*, 109–115.

(17) Ali, F. E.; Bondinell, W. E.; Dandridge, P. A.; Frazee, J. S.; Garvey, E.; Girard, G. R.; Kaiser, C.; Ku, T. W.; Lafferty, J. J.; Moonsammy, G. I.; Oh, H.-J.; Rush, J. A.; Setler, P. E.; Stringer, O. D.; Venslavsky, J. W.; Volpe, B. W.; Yunger, L. M.; Zirkle, C. L. Orally active and potent inhibitors of γ-aminobutyric acid uptake. *J. Med. Chem*. **1985**, *28*, 653–660.

(18) Dalby, N. O. GABA-level increasing and anticonvulsant effects of three different GABA uptake inhibitors. *Neuropharmacology* **2000**, *39*, 2399–2407.

(19) Borden, L. A.; Dhar, T. G. M.; Smith, K. E.; Weinshank, R. L.; Branchek, T. A.; Gluchowski, C. Tiagabine, SK&F 89976-A, CI-966, and NNC-711 are selective for the cloned GABA transporter GAT-1. *Eur. J. Pharmacol.* **1994**, *269*, 219–224.

(20) Frey, H.-H.; Popp, C.; Loescher, W. Influence of the inhibitors of high affinity GABA uptake on seizure threshold in mice. *Neuropharmacology* **1979**, *18*, 581–590.

(21) Genton, P.; Guerrini, R.; Perucca, E. Tiagabine in clinical practice. *Epilepsia* **2001**, *42*, 42–45.

(22) Salat, K.; Podkowa, A.; Malikowska, N.; Kern, F.; Pabel, J.; Wojcieszak, E.; Kulig, K.; Wanner, K. T.; Strach, B.; Wyska, E. Novel, highly potent and *in vivo* active inhibitor of GABA transporter subtype 1 with anticonvulsant, anxiolytic, antidepressant and antinociceptive properties. *Neuropharmacology* **2017**, *113*, 331–342.

(23) Müller-Uri, C.; Singer, E. A.; Fleischhacker, W. Synthesis of alkyl-substituted arecoline derivatives as γ-aminobutyric acid uptake inhibitors. *J. Med. Chem*. **1986**, *29*, 125–132.

(24) Lapuyade, G.; Schlewer, G.; N'Goka, V.; Vernieres, J.-C.; Chambon, J.-P.; Lagrange, J.; Lagrange, P.; Wermuth, C. G. Alkyl and aryl derivatives of nipecotic acid: synthesis and inhibition of GABA uptake as a function of conformational parameters and bioavailability. *Eur. J. Med. Chem.* **1987**, *22*, 383–391.

(25) N'Goka, V.; Schlewer, G.; Linget, J.-M.; Chambon, J.-P.; Wermuth, C. G. GABA-uptake inhibitors: construction of a general pharmacophore model and successful prediction of a new representative. *J. Med. Chem*. **1991**, *34*, 2547–2557.

(26) Hoesl, C. E.; Höfner, G.; Wanner, K. T. First asymmetric syntheses of 6-substituted nipecotic acid derivatives. *Tetrahedron* **2004**, *60*, 307–318.

(27) N'Goka, V.; Bissantz, C.; Bisel, P.; Stenbøl, T. B.; Krogsgaard-Larsen, P.; Schlewer, G. Syntheses and GABA uptake properties of 6-ether- and 6-enol ether-substituted nipecotic acids. *Eur. J. Med. Chem.* **2004**, *39*, 633–638.

(28) N'Goka, V.; Stenbøl, T. B.; Krogsgaard-Larsen, P.; Schlewer, G. Synthesis and GABA uptake inhibitory properties of 6-aryl iminoxymethyl substituted nipecotic acids. *Eur. J. Med. Chem.* **2004**, *39*, 889–895.

(29) Hellenbrand, T.; Höfner, G.; Wein, T.; Wanner, K. T. Synthesis of 4-substituted nipecotic acid derivatives and their evaluation as potential GABA uptake inhibitors. *Bioorg. Med. Chem*. **2016**, *24*, 2072–2096.

(30) Yamashita, A.; Singh, S. K.; Kawate, T.; Jin, Y.; Gouaux, E. Crystal structure of a bacterial homologue of Na^+/Cl^--dependent neurotransmitter transporters. *Nature* **2005**, *437*, 1–9.

(31) Palló, A.; Bencsura, Á.; Héja, L.; Beke, T.; Perczel, A.; Kardos, J.; Simon, Á. Major human γ-aminobutyrate transporter: *in silico* prediction of substrate efficacy. *Biochem. Biophys. Res. Commun.* **2007**, *364*, 952–958.

(32) Wein, T.; Wanner, K. T. Generation of a 3D model for human GABA transporter hGAT-1 using molecular modeling and investigation of the binding of GABA. *J. Mol. Model.* **2010**, *16*, 155–161.

(33) Skovstrup, S.; Taboureau, O.; Bräuner-Osborne, H.; Jørgensen, F. S. Homology modelling of the GABA transporter and analysis of tiagabine binding. *ChemMedChem* **2010**, *5*, 986–1000.

(34) Wein, T.; Petrera, M.; Allmendinger, L.; Höfner, G.; Pabel, J.; Wanner, K. T. Different binding modes of small and large binders of GAT1. *ChemMedChem* **2016**, *11*, 509–518.

(35) Sindelar, M.; Wanner, K. T. Library screening by means of MS Binding Assays – exemplarily demonstrated for a pseudo-static library addressing GAT1. *ChemMedChem* **2012**, *7*, 1678–1690.

(36) Höfner, G.; Wanner, K. T. Competitive binding assays made easy with a native marker and mass spectrometric quantification. *Angew. Chem. Int. Ed*. **2003**, *42*, 5235–5237.

(37) Höfner, G.; Zepperitz, C.; Wanner, K. T. MS Binding Assays – An Alternative to Radioligand Binding. In *Mass Spectrometry in Medicinal Chemistry: Applications in Drug Discovery*, 1st ed.; Höfner, G., Wanner, K. T., Eds.; Wiley-VCH: Weinheim, 2007; pp 247–283.

(38) Zepperitz, C.; Höfner, G.; Wanner, K. T. MS-Binding Assays: kinetic, saturation and competitive experiments based on quantitation of bound marker – exemplified by the GABA transporter mGAT1. *ChemMedChem* **2006**, *1*, 208–217.

(39) Petrera, M.; Wein, T.; Allmendinger, L.; Sindelar, M.; Pabel, J.; Höfner, G.; Wanner, K. T. Development of highly potent GAT1 inhibitors: synthesis of nipecotic acid derivatives by Suzuki-Miyaura cross-coupling reactions. *ChemMedChem* **2016**, *11*, 519–538.

(40) Lutz, T.; Wein, T.; Höfner, G.; Wanner, K. T. Development of highly potent GAT1 inhibitors: synthesis of nipecotic acid derivatives with *N*-arylalkynyl substituents. *ChemMedChem* **2017**, *12*, 362–371.

(41) A synthesis of *rac*-**23** excluding analytical data is described in: Binch, H.; Hashimoto, M.; Mortimore, M.; Ohkubo, M.; Sunami, T. Novel Aminopyridine Derivatives Having Aurora Selective Inhibitory Action. Patent US 2012/0015969 A1, Jan 1, 2012.

(42) A synthesis of **25** excluding analytical data is described in: Durón, S.; Campbell, D.; Ndubaku, C.; Rudolph, J. Serine/Threonine Kinase Inhibitors. Patent US 2014/0323478 A1, Oct 30, 2014.

(43) Smith, A. B.; Kim, D.-S. A general, convergent strategy for the construction of indolizidine alkaloids: total syntheses of (-)-indolizidine 223AB and alkaloid (-)-205B. *J. Org. Chem*. **2006**, *71*, 2547–2557.

(44) For chiral pool syntheses of enantiopure (3*S*,5*R*)-**20** (excluding analytical data) and enantiopure (3*S*,5*R*)-**27** (including analytical data) see: Mori, Y.; Iwamoto, M.; Mori, K.; Yoshida, M.; Honda, T.; Nagayama, T.; Nishi, T. An efficient synthesis of (3*S*,5*S*)-5-[3,3-

dimethyl-1-(*o*-tolyl)-6-oxo-2*H*-pyridin-4-yl]piperidine-3-carboxamide as potent renin inhibitor. *Heterocycles* **2014**, *89*, 1413−1426.

(45) Brosse, N.; Pinto, M.-F.; Jamart-Grégoire, B. *N-tert*-Butoxycarbonylaminophthalimide, a versatile reagent for the conversion of alcohols into alkylated *tert*-butylcarbazates or hydrazines via the Mitsunobu protocol. *Tetrahedron Lett.* **2000**, *41*, 205−207.

(46) Brosse, N.; Pinto, M.-F.; Jamart-Grégoire, B. New synthesis of 1,1-substituted hydrazines by alkylation of *N*-acyl- or *N*-alkyloxycarbonylaminophthalimide using the Mitsunobu protocol. *J. Org. Chem.* **2000**, *65*, 4370−4374.

(47) Brosse, N.; Pinto, M.-F.; Jamart-Grégoire, B. Preparation of multiply protected alkylhydrazine derivatives by Mitsunobu and PTC approaches. *Eur. J. Org. Chem*. **2003**, *2003* 4757−4764.

(48) For asymmetric syntheses (including analytical data) of enantiopure (3*R*,5*R*)-**28** and enantiopure (3*S*,5*S*)-**28** see: Iding, H.; Wirz, B.; Sarmiento, R.-M. R. Chemoenzymatic preparation of non-racemic *N*-Boc-piperidine-3,5-dicarboxylic acid 3-methyl esters and their 5-hydroxylmethyl derivatives. *Tetrahedron: Asymmetry* **2003**, *14*, 1541−1545.

(49) General note on hydrazine stability: The hydrazines *rac*-**11**–*rac*-**14** were prone for degradation, presumably to give corresponding hydrocarbons analogous to the observations in: Hoffman, R. V.; Kumar, A. Oxidation of hydrazine derivatives with arylsulfonyl peroxides. *J. Org. Chem*. **1984**, *49*, 4014–4017. The hydrazines were thus isolated and used in further experiments as their more stable hydrochlorides. As shown by elemental analysis, all hydrazines were obtained with 3 equivalents of HCl and 1 equivalent of H_2O with exception of hydrazine *rac*-**11**, which had 2 equivalents HCl and 1 H_2O. We performed control experiments in order to demonstrate that neither the use as hydrochloride nor the low hydrazine stability itself would affect the outcome of the screening experiments (data not shown). The buffer capacity in the bioassays was high enough to neutralize the HCl without affecting the pH. To guarantee hydrazine and hydrazone stability throughout the screening experiments the antioxidant sodium L-ascorbate (200 μM) was added to the incubation buffer.

(50) Fujimoto, T.; Imaeda, Y.; Konishi, N.; Hiroe, K.; Kawamura, M.; Textor, G. P.; Aertgeerts, K.; Kubo, K. Discovery of a tetrahydropyrimidin-2(1*H*)-one derivative (TAK-

442) as a potent, selective, and orally active factor Xa inhibitor. *J. Med. Chem*. **2010**, *53*, 3517−3531.

(51) Sindelar, M.; Lutz, T. A.; Petrera, M.; Wanner, K. T. Focused pseudostatic hydrazone libraries screened by mass spectrometry binding assay: optimizing affinities toward γ-aminobutyric acid transporter 1. *J. Med. Chem*. **2013**, *56*, 1323−1340.

(52) Kern, F. T.; Wanner, K. T. Generation and screening of oxime libraries addressing the neuronal GABA transporter GAT1. *ChemMedChem* **2015**, *10*, 396−410.

(53) Irngartinger, H.; Escher, T. Strong electron acceptor properties of 3'-(pentafluorophenyl)isoxazolol[4',5':1,2][60]fullerene derivatives. *Tetrahedron* **1999**, *55*, 10753−10760.

(54) Likewise the hydrazines,[49] also the corresponding hydrazones (*rac*-**16**−*rac*-**19**) showed a low stability. The hydrazones were thus prepared in 10 mM solutions, in which they were directly used for full-scale competition experiments without additional drying or purification. The reactions were performed in deuterated solvents to demonstrate completeness of hydrazone formation by NMR and structures of the hydrazones in solution were confirmed by ^{1}H and ^{13}C NMR and HRMS prior to their use in the bioassays.

Sodium deuteroxide was used to neutralize the hydrazine hydrochlorides and thus sodium chloride was obtained as side product (2 equivalents NaCl for *rac*-**16** and 3 equivalents NaCl for *rac*-**18**), which was not separated. We consider the presence of NaCl in the sample as negligible for the outcome of the bioassays; in the bioassays incubation buffers typically contain high salt concentrations and thus the additional, low-concentrated NaCl from the test substance is insignificant.

(55) Kragler, A.; Höfner, G.; Wanner, K. T. Synthesis and biological evaluation of aminomethylphenol derivatives as inhibitors of the murine GABA transporters mGAT1–GAT4. *Eur. J. Med. Chem*. **2008**, *43*, 2404–2411.

(56) Steffan, T.; Renukappa-Gutke, T.; Höfner, G.; Wanner, K. T. Design, synthesis and SAR studies of GABA uptake inhibitors derived from 2-substituted pyrrolidine-2-ylacetic acids. *Bioorg. Med. Chem*. **2015**, *23*, 1284–1306.

(57) Tsuruda, P. R.; Yung, J.; Martin, W. J.; Chang, R.; Mai, N.; Smith, J. A. M. Influence of ligand binding kinetics on functional inhibition of human recombinant serotonin and norepinephrine transporters. *J. Pharmacol. Toxicol. Methods* **2010**, *61*, 192–204.

(58) Hulme, E. C.; Trevethick, M. A. Ligand binding assays at equilibrium: validation and interpretation. *Br. J. Pharmacol*. **2010**, *161*, 1219–1237.

(59) Sarup, A.; Larsson, O. M.; Bolvig, T.; Frølund, B.; Krogsgaard-Larsen, P.; Schousboe, A. Effects of 3-hydroxy-4-amino-4,5,6,7-tetrahydro-1,2-benzisoxazol (*exo*-THPO) and its N-substituted analogs on GABA transport in cultured neurons and astrocytes and by the four cloned mouse GABA transporters. *Neurochem. Int*. **2003**, *43*, 445–451.

(60) Clausen, R. P.; Moltzen, E. K.; Perregaard, J.; Lenz, S. M.; Sanchez, C.; Falch, E.; Frølund, B.; Bolvig, T.; Sarup, A.; Larsson, O. M.; Schousboe, A.; Krogsgaard-Larsen, P. Selective inhibitors of GABA uptake: synthesis and molecular pharmacology of 4-*N*-methylamino-4,5,6,7-tetrahydrobenzo[*d*]isoxazol-3-ol analogues. *Bioorg. Med. Chem*. **2005**, *13*, 895–908.

(61) White, H. S.; Watson, W. P.; Hansen, S. L.; Slough, S.; Perregaard, J.; Sarup, A.; Bolvig, T.; Petersen, G.; Larsson, O. M.; Clausen, R. P.; Frølund, B.; Falch, E.; Krogsgaard-Larsen, P.; Schousboe, A. First demonstration of a functional role for central nervous system betaine/γ-aminobutyric acid transporter (mGAT2) based on synergistic

anticonvulsant action among inhibitors of mGAT1 and mGAT2. *J. Pharmacol. Exp. Ther.* **2005**, *312*, 866–874.

(62) Timple, J. M. V.; Magalhães, L. G.; Souza Rezende, K. C.; Pereira, A. C.; Cunha, W. R.; Andrade e Silva, M. L.; Mortensen, O. V.; Fontana, A. C. K. The lignan (-)-hinokinin displays modulatory effects on human monoamine and GABA transporter activities. *J. Nat. Prod.* **2013**, *76*, 1889−1895.

(63) Christopoulos, A.; Changeux, J.-P.; Catterall, W. A.; Fabbro, D.; Burris, T. P.; Cidlowski, J. A.; Olsen, R. W.; Peters, J. A.; Neubig, R. R.; Pin, J.-P.; Sexton, P. M.; Kenakin, T. P.; Ehlert, F. J.; Spedding, M.; Langmead, C. J. International Union of Basic and Clinical Pharmacology. XC. multisite pharmacology: recommendations for the nomenclature of receptor allosterism and allosteric ligands. *Pharmacol. Rev*. **2014**, *66*, 918−947.

(64) Schmitt, S.; Höfner, G.; Wanner, K. T. MS Transport Assays for γ-aminobutyric acid transporters – an efficient alternative for radiometric assays. *Anal. Chem*. **2014**, *86*, 7575–7583.

(65) Schmitt, S.; Höfner, G.; Wanner, K. T. Application of MS Transport Assays to the four human γ-aminobutyric acid transporters. *ChemMedChem* **2015**, *10*, 1498–1510.

(66) Kragholm, B.; Kvist, T.; Madsen, K. K.; Jørgensen, L.; Vogensen, S. B.; Schousboe, A.; Clausen, R. P.; Jensen, A. A.; Bräuner-Osborne, H. Discovery of a subtype selective inhibitor of the human betaine/GABA transporter 1 (BGT-1) with a non-competitive pharmacological profile. *Biochem. Pharmacol*. **2013**, *86*, 521–528.

(67) Changeux, J.-P. The nicotinic acetylcholine receptor: a typical 'allosteric machine'. *Phil. Trans. R. Soc. B* **2018**, *373*, 20170174.

(68) Ballatore, C.; Huryn, D. M.; Smith, A. B., 3rd. Carboxylic acid (bio)isosteres in drug design. *ChemMedChem* **2013**, *8*, 385–395.

(69) Lassalas, P.; Gay, B.; Lasfargeas, C.; James, M. J.; Tran, V.; Vijayendran, K. G.; Brunden, K. R.; Kozlowski, M. C.; Thomas, C. J.; Smith, A. B., 3rd; Huryn, D. M.; Ballatore, C. Structure property relationships of carboxylic acid isosteres. *J. Med. Chem.* **2016**, *59*, 3183–3203.

(70) Merck, E. *Anfärbereagenzien für Dünnschicht- und Papier-Chromatographie*; MERCK: Darmstadt, 1970.

(71) Cushman, M.; Georg, G. I.; Holzgrabe, U.; Wang, S. Absolute quantitative ^{1}H NMR spectroscopy for compound purity determination. *J. Med. Chem*. **2014**, *57*, 9219.

(72) Pauli, G. F.; Chen, S. N.; Simmler, C.; Lankin, D. C.; Godecke, T.; Jaki, B. U.; Friesen, J. B.; McAlpine, J. B.; Napolitano, J. G. Importance of purity evaluation and the potential of quantitative ^{1}H NMR as a purity assay. *J. Med. Chem*. **2014**, *57*, 9220−9231.

(73) Aldrich, C.; Bertozzi, C.; Georg, G. I.; Kiessling, L.; Lindsley, C.; Liotta, D.; Merz, K.; M.; Schepartz, A.; Wang, S. The ecstasy and agony of assay interference compounds. *J. Med. Chem.* **2017**, *60*, 2165−2168.

(74) Sterling, T.; Irwin, J. J. ZINC 15 – ligand discovery for everyone. *J. Chem. Inf. Model.* **2015**, *55*, 2324−2337.

(75) Peaks for the protons of OH and NH groups disappeared due to deuterium exchange. In the ^{1}H NMR spectra of compounds *rac*-**23**, *rac*-**27**, *rac*-**28**, *rac*-**32**, *rac*-**11**, *rac*-**12**, *rac*-**37**, (partly) *rac*-**38**, *rac*-**13**, *rac*-**14** and all hydrazones *rac*-**16** or *rac*-**18** no corresponding signals were detectable.

(76) In addition to the signals listed ^{1}H NMR and ^{13}C NMR (and if applicable ^{19}F NMR) spectra showed signals of low intensity (3−17%) corresponding to the *Z*-isomer.

(77) Zepperitz, C.; Höfner, G.; Wanner, K. T. Expanding the scope of MS Binding Assays to low-affinity markers as exemplified for mGAT1. *Anal. Bioanal. Chem*. **2008**, *391*, 309–316.

(78) Cheng, Y. C.; Prussoff, W. H. Relationship between the inhibition constant (K_i) and the concentration of inhibitor which causes 50 per cent inhibition (IC_{50}) of an enzymatic reaction. *Biochem. Pharmacol*. **1973**, *22*, 3099–3108.

Table of Contents Graphic